DEPARTMENT OF AEROSPACE ENGINEERING
COLLEGE OF ENGINEERING AND TECHNOLOGY
OLD DOMINION UNIVERSITY
NORFOLK, VIRGINIA 23529-0247

# MAGNETIC SUSPENSION TECHNOLOGY DEVELOPMENT

**By**
Dr. Colin Britcher, Principal Investigator
Department of Aerospace Engineering

**FINAL REPORT**
For the period January 1, 1997 through May 31, 1998

**Prepared for**
NASA Langley Research Center
Guidance and Control Branch,
Flight Dynamics and Control Division
Attn.: Nelson J. Groom
Technical Officer
Mail Stop 161
Hampton, VA 23681-0001

**Under**
NASA Grant No. NCC1-248
ODURF Project No. 170051

**August 1998**

DEPARTMENT OF AEROSPACE ENGINEERING
COLLEGE OF ENGINEERING AND TECHNOLOGY
OLD DOMINION UNIVERSITY
NORFOLK, VIRGINIA 23529-0247

# MAGNETIC SUSPENSION TECHNOLOGY DEVELOPMENT

**By**
Dr. Colin Britcher, Principal Investigator
Department of Aerospace Engineering

**FINAL REPORT**
For the period January 1, 1997 through May 31, 1998

**Prepared for**
NASA Langley Research Center
Guidance and Control Branch,
Flight Dynamics and Control Division
Attn.: Nelson J. Groom
Technical Officer
Mail Stop 161
Hampton, VA 23681-0001

**Under**
NASA Grant No. NCC1-248
ODURF Project No. 170051

**Submitted by**
Old Dominion University Research Foundation
800 West 46th Street
Norfolk, VA 23508

**August 1998**

# MAGNETIC SUSPENSION TECHNOLOGY DEVELOPMENT

A Final Report for Cooperative Agreement NCC-1-248 between
NASA Langley Research Center and Old Dominion University

Principal Investigator - Dr. Colin P. Britcher, Department of Aerospace Engineering

For attention of Nelson J. Groom
Guidance and Control Branch, Flight Dynamics and Control Division, MS 161

For Period January 1, 1997 thru May 31, 1998

## SUMMARY

This Cooperative Agreement, intended to support focused research efforts in the area of magnetic suspension systems, was initiated between NASA Langley Research Center (LaRC) and Old Dominion University (ODU) starting January 1, 1997. The original proposal called for a three-year effort, but funding for the second year proved to be unavailable, leading to termination of the agreement following a 5-month no-cost extension. This report covers work completed during the entire 17-month period of the award.

This research built on work that had taken place over recent years involving both NASA LaRC and the Principal Investigator (PI). The research was of a rather fundamental nature, although specific applications were kept in mind at all times, such as wind tunnel Magnetic Suspension and Balance Systems (MSBS), space payload pointing and vibration isolation systems, magnetic bearings for unconventional applications, magnetically levitated ground transportation and electromagnetic launch systems. Fundamental work was undertaken in areas such as the development of optimized magnetic configurations, analysis and modelling of eddy current effects, control strategies for magnetically levitated wind tunnel models and system calibration procedures.

Despite the termination of this Cooperative Agreement, several aspects of the research work are currently continuing with alternative forms of support.

## INTRODUCTION

Research over recent years in the Guidance and Control Branch (formerly the Spacecraft Controls Branch) has been aimed towards the development of new technologies and applications for magnetic suspension systems. Most notable, perhaps, has been the development of systems with a capability for large angular displacements, also with large air gaps between suspension electromagnets and the suspended object. Two small-scale proof-of-concept test fixtures had been completed, with a much larger system, the Large Gap Magnetic Suspension System (LGMSS), due to be commissioned late in 1998. Other previous work at LaRC had examined the application of small air-gap technology to various space applications, including momentum storage/exchange devices and payload pointing/vibration isolation systems and on the development and use of magnetic suspension and balance systems for wind tunnel models.

## SUMMARY OF NASA EQUIPMENT AND RESOURCES USED IN THE EXECUTION OF THIS COOPERATIVE AGREEMENT

A suite of computer codes, licensed to LaRC and known as OPERA, VF/GFUN, TOSCA and ELEKTRA, have been extensively used. The magnetic suspension laboratory in Building 1232, which houses the two large-angle test fixtures previously mentioned has been used for the system modelling and eddy current analysis work. Frequent consultations occured between the PI and students working under this Cooperative Agreement and personnel at LaRC, principally those from GCB, FDCD.

## SUMMARY OF ODU EQUIPMENT AND RESOURCES USED IN THE EXECUTION OF THIS COOPERATIVE AGREEMENT

ODU acquired a licence for the 2-D version of the OPERA software package, which has been used for some verification work. An early phase of the Cooperative Agreement work involved operation of the Annular Suspension and Pointing System (ASPS), which was previously loaned to ODU by LaRC following around a decade in storage. The system was recommissioned by successive teams of undergraduate and graduate students and is now operational with new power supplies and a digital controller.

## DESCRIPTION OF WORK COMPLETED UNDER THE COOPERATIVE AGREEMENT

### A - Design Optimization of Magnetic Suspension Systems

This is an area where little was known, but the potential for advance was seen to be great. The electromagnet configurations of large-gap magnetic suspension systems has traditionally been developed based on the skill and experience of the designer, coupled with an exceedingly limited application of "optimization" methods, almost universally in an ad hoc, trial-and-error fashion. In recent years, powerful general purpose optimization codes have been developed and made available in a relatively user-friendly form. It was realized that the design of magnetic suspension sytems could be approached in a much more systematic and rigorous manner than in the past, provided sensible optimization criteria could be defined and the relevant governing equations organized in a relatively simple way. David Cox, of GCB, FDCD showed that these requirements can be met, and had demonstrated the possibility of optimization of simple large-gap configurations, with promising results. The "optimum" configurations (based on minimum power or maximum controllability for example) differed significantly from the configurations in use, which were derived following more traditional methods. It is felt that as configurations became more complex, the wind tunnel MSBS application perhaps being the most notable, the potential for design "breakthroughs", i.e. dramatic improvements in system design and performance, would become greater. Small-gap, bearing-type systems are relatively less complex from the point of view of magnetic configurations, so are probably less likely to be far from optimal configurations as currently used. Indeed, elementary optimization by analytic manipulation of magnetic circuit equations is possible in simple cases. However, where additional complexity is added, such as magnetic material saturation, anisoptropy, or geometrical constraints, there exists a need for systematic optimization procedures able to refine the standard configurations.

Progress under the period of this Cooperative Agreement can be summarized by the material included as Appendix A of this report, which was presented as an AIAA student paper in 1997 (Reference 2). The paper won 3rd place in the graduate category. Later work by the same author, leading towards a Masters thesis expected in August 1998, was carried out under NASA GSRP support and will not be discussed further here.

B - Wind Tunnel MSBSs

At the time of the initiation of the Cooperative agreement, there were no ongoing wind tunnel MSBS development efforts known within the U.S. A variety of proposals were prepared in collaboration with personnel from GCB, FDCD and FSED, NASA LaRC for in-house programs, with no success. However, an initiative spearheaded by Princeton University, with support from the Office of Naval Research, was showing promise, and became the technical focus for work under the Cooperative Agreement. The application is to an ultra-high Reynolds number wind tunnel, exploiting high pressures in the working fluid, and appears to be technically feasible with more-or-less current technology. Some preliminary work has been undertaken in support of this project, and will now be discussed briefly.

A general review of the new application was prepared and reported as Reference 3, included here as Appendix B, drawing on some material presented earlier as Reference 1, included here as Appendix C. It was concluded that the application was generally feasible, but with some critical issues demanding attention, perhaps notably the compatibility of the MSBS with the steel pressure shell required for the wind tunnel. A secondary issue was the provision of roll control for the suspended element, which has been a long-standing historical problem in MSBS development.

A new transverse magnetization concept was studied, drawing on results from the laboratory-scale test fixtures mentioned earlier. Here, the magnetic core, placed in the aerodynamic model's fuselage as usual, is magnetized vertically, instead of axially as has been the universal practice. The thinking here is that large rolling moments can be generated with this new design; a well-known weakness with the traditional configuration. The governing equations for force and moment production are similar in both cases :

$$F \approx Vol(M_x.\nabla B);\ T \approx Vol(M_x \times B) \qquad (axial\ magnetization)$$
$$F \approx Vol(M_z.\nabla B);\ T \approx Vol(M_z \times B) \qquad (vertical\ magnetization)$$

Careful inspection reveals that no torque can be generated by the cross product terms in one degree-of-freedom in either case; namely roll with axial magnetization and yaw with vertical magnetization. Torques in this degree-of-freedom can be generated by a variety of other means, including a gradient of a transverse force via terms such as :

$$T \approx \int_{length} M_z.B_{yz}\, dVol \qquad (vertical\ magnetization)$$

This term can be made relatively large if the magnetization is perpendicular to the long axis of a slender magnetic core, and an axial gradient in the applied field, $B_{xyz}$ is created. The details of analysis carried out under the Cooperative Agreement is presented in Reference 6. This document is not reproduced here since it is readily available.

C - System Modelling

Considerable strides have been made over the past few years concerning various aspects of the modelling of magnetic suspension systems. One of the most notable areas are the development of dynamic models which properly incoporate eddy current effects, which had previously been largely ignored or overlooked. This work predates the Cooperative

Agreement, but continued throughout. Fundamanetal developments are summarized in Reference 7. This document is not reproduced here since it is readily available. Here, considerable use needed to be made of the LaRC-licensed code ELEKTRA.

An immediate application of these generic results is to the development of a dynamic model of the LGMSS, due to come on-line late this year or early next year. Soem analysis has been undertaken but will be reported separately.

D - Payload Pointing and Vibration Isolation

Application of the ASPS approach to the problem of fine pointing and vibration isolation of large space payloads is still of some interest. Revised control software for the ASPS hardware at ODU was developed under a previous Grant and demonstrated during the early phases of the Cooperative Agreement. Full details were reported in the semi-annual progress report, based on Reference 4, and will not be reproduced here due to space limitations.

F - Symposia

The PI served at the Technical Program Co-Chair for the successful 1997 International Symposium on Magnetic Suspension Technology, held in Gifu City, Japan, in collaboration with the National Aerospace Laboratory (NAL). Over 40 papers were presented. The Proceedings have since been editied and published as NASA CP-1998-207654, May 1998. The 1999 meeting is tentatively set for the University of California, Santa Barbara, in December 1999.

G - Other areas - the Backers Bearing

Due to needs arising from a separate project, the PI was asked to examine some aspects of the performance of the "Backers" baring concept, using the OPERA/TOSCA software. The attraction of the Backers configuration is that it achieves passive stability in repulsion from arrays of alternating-polarity permanent magnets. Some analysis was undertaken, although the results cannot be considered fully complete at this time. However, due to its perceived importance, the material developed is presented herein as Appendix D.

## PERSONNEL

Three graduate students were involved at various times during the period of this Cooperative Agreement. Yan Yang completed her Masters degree in Aerospace Engineering in December 1997 and is now employed at Honeywell Corporation. Dale Bloodgood worked under the Cooperative Agreement and subsequently transitioned to support under a NASA GSRP, as previously mentioned. He is expected to complete his Masters degree requirements in Engineering Mechanics in August 1998. The third student was Oscar Gomeiz, a Masters student of Aerospace Engineering, who is expected to graduate in May 1999, focusing on the Princeton MSBS project.

## PUBLICATIONS AND PRESENATIONS DURING THE COOPERATIVE AGREEMENT

1. Britcher, C.P.: Application of magnetic suspension technology to large scale facilities. Presented at AIAA 35th Aerospace Sciences meeting, Reno, NV, January 1997. AIAA 97-0346

2. Bloodgood, D.V.: Optimization of force and efficiency of iron core electromagnets. Presented at the AIAA Regional Student Paper Competition, Norfolk, VA, April, 1997. (3rd place, graduate student category).

3. Britcher, C.P.: Provision of support interference free static and dynamic test capability in high Reynolds number facilities. Presented at the Workshop on Needs for High Reynolds Number Facilities to Design the Next Generation of Sea and Air Vehicles, Arlington, VA, June 1997.

4. Yang, Y.: Research related to multi degree-of-freedom magnetic suspensions. Masters thesis, Old Dominion University, August 1997. Also submitted as a Progress Report under NCC-1-248.

5. Britcher, C.P.: Opportunities for application of superconducting magnet technology to large gap magnetic suspensions. 10th International Symposium on Superconductivity, Gifu City, Japan, October 1997.

6. Britcher, C.P.: Wind tunnel magnetic suspension and balance systems with vertically magnetized model cores. 4th International Symposium on Magnetic Suspension Technology, Gifu City, Japan, November 1997. Published as NASA CP-1998-207654, May 1998.

7. Britcher, C.P.; Bloodgood, D.V.: Eddy current influences on the dynamic behaviour of magnetic suspension systems. 4th International Symposium on Magnetic Suspension Technology, Gifu City, Japan, November 1997. Published as NASA CP-1998-207654, May 1998.

Appendix A

Bloodgood, D.V.: Optimization of force and efficiency of iron core electromagnets. Presented at the AIAA Regional Student Paper Competition, Norfolk, VA, April, 1997.

## ABSTRACT

This paper discusses the optimization of the force and efficiency of radially symmetric, iron-cored electromagnets. The equations for the magnetic force and power consumption are derived from first principles. Discussions focus on the derivation of the governing equations and the interpretation of the optimization results. The intent is to uncover and define the controlling trends associated with the efficient generation of magnetic force.

## INTRODUCTION

The specific goals of this research are to further the understanding of electromagnetic force production and to optimize electromagnet designs. Specifically, the optimization of the magnetic force and force per unit power. The models used in this paper have been kept as general as possible making the results applicable to standard materials and devices as well as newer experimental materials. Because of differences in material properties and construction methods the results discussed will focus on trends rather then specific values. The optimization process was carried out as a three-step process. The steps included the development of the governing equations from first principles, the actual optimization of the modelling equations, and the interpretation of results. These results should increase the efficiency and commercial viability of many magnetic technologies including wind tunnel model suspension and balance systems, space payload pointing and vibration isolation systems, satellite momentum storage and control devices, maglev trains, and electromagnet launch systems.

$$F = \frac{B^2 A_g}{2\mu_0} \tag{2}$$

The magnetic flux density B is related to the magnetic field intensity in air by,

$$B = \mu_0 H \tag{3}$$

The magnetic flux in a material is defined as the magnetic flux density multiplied by the area through which it flows. Therefore the flux of the individual materials can be written out as,

$$\begin{aligned} \phi_g &= B_g A_g = \mu_0 \mu_g H_g A_g \\ \phi_{FE} &= B_{FE} A_{FE} = \mu_0 \mu_{FE} H_{FE} A_{FE} \\ \phi_S &= B_S A_S = \mu_0 \mu_S H_S A_S \end{aligned} \tag{4}$$

Combining Eq. (3) and Eq. (4) makes it possible to write the magnetic flux within the iron section and the surface section in terms of the flux in the air gap.

$$\begin{aligned} \mu_0 \mu_{FE} H_{FE} A_{FE} &= \mu_0 \mu_g H_g A_g \\ \mu_0 \mu_S H_S A_S &= \mu_0 \mu_g H_g A_g \end{aligned} \tag{5}$$

Rearranging these equations the magnetic field intensities for the iron and the magnetic surface can be written in terms of the magnetic field intensity of the air gap.

$$H_{FE} = H_g\left(\frac{A_g}{A_{FE}}\right)\left(\frac{\mu_g}{\mu_{FE}}\right)$$
$$H_S = H_g\left(\frac{A_g}{A_S}\right)\left(\frac{\mu_g}{\mu_S}\right) \qquad (6)$$

The next step in the derivation is to introduce the magnetic field intensity equations into the magnetomotive force equation, Eq. (7). The equation is given below where N equals the number of turns in the coil and I represents the current running through the wire. The combined term NI is defined as the ampere turns.

$$NI = \oint \vec{H}\cdot d\vec{L} = \sum_{i=1}^{n} (H_i L_i) \qquad (7)$$

The line integral follows a path of the magnetic flux produced by the current loops. For the case of a simple electromagnet the magnetic flux would travel through the iron core of the magnet, across the air gap, through the material that the magnet is acting on, and then across the second air gap before returning to the iron core. Substituting these values into the summation results in the following expression for NI,

$$NI = 2(H_g L_g) + (H_{FE} L_{FE}) + (H_S L_S) \qquad (8)$$

Substituting Eq. (6) into Eq. (8) yields,

$$NI = H_g\left[2L_g + \frac{L_{FE} A_g \mu_g}{A_{FE}\mu_{FE}} + \frac{L_S A_g \mu_g}{A_S \mu_S}\right] \qquad (9)$$

Rearranging terms results in an equation for the magnetic flux passing across the air gap.

$$H_g = \frac{NI}{(2L_g + \frac{L_{FE} A_g \mu_g}{A_{FE} \mu_{FE}} + \frac{L_S A_g \mu_g}{A_S \mu_S})} \tag{10}$$

Assuming $\mu_{FE} >> \mu_g$ and $\mu_S >> \mu_g$, Eq. (10) simplifies to,

$$H_g \approx \frac{1}{2}(\frac{NI}{L_g}) \tag{11}$$

The electromagnetic force equation can now be rewritten in terms of the physical parameters NI, $L_g$, and $\mu_g$. Substitute Eq. (11) into Eq. (3), and then substitute this result into Eq. (2) yields,

$$F = \frac{(\mu_0 H_g)^2 A_g}{2\mu_0} = (\frac{\mu_0 NI}{2L_g})^2 \frac{A_g}{2\mu_0} = \frac{\mu_0 (NI)^2 A_g}{8L_g^2} \tag{12}$$

The value of NI defining the magnetomotive force can be rewritten as,

$$NI = (I_d)(A_c) \tag{13}$$

Where $A_c$ is the cross sectional area of the coil windings. Substituting Eq. (13) into Eq. (12) gives the electromagnetic force equation in terms of the physical parameters of the coil.

$$F = \frac{\mu_0 I_d^2 A_C^2 A_g}{8L_g^2} \tag{14}$$

This is the equation that will be used to optimize the force produced by an electromagnetic coil per unit power, weight, volume, and so on. $A_g$ represents the area of the iron surface exposed to the material that the electromagnet is acting on. $A_c$ represents the cross sectional area of the coil windings.

## DERIVATION OF POWER EQUATION

The derivation of the force equation was done for the most general case possible. It is possible to do the same for the derivation of the power equation but it does not lead to an easy understanding of the process. Because of this the power equations will be derived using the specific coil design which is being optimized. For this case it is a radially symmetric cylindrical coil, shown in **Fig. 2**. A cross sectional view is shown in **Fig. 3**.

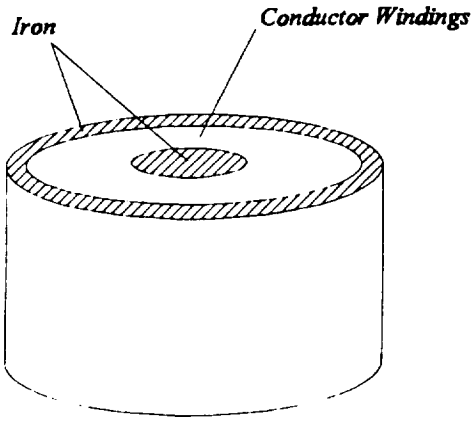


**Figure 2: Radially symmetric coil.**

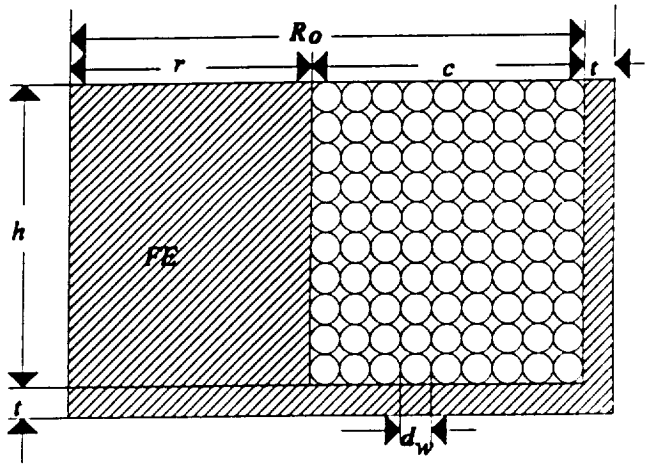


**Figure 3: Cross section of coil.**

**Nomenclature**

| | | | |
|---|---|---|---|
| P= Power | (watts) | I= Current | (amps) |
| R= Resistance | (ohms) | ρ= Wire Resistivity | (ohm mm) |
| $A_w$= Area of wire | ($mm^2$) | $L_w$= Length of wire | (mm) |
| $d_w$= Diameter of wire | (mm) | $V_c$= Volume of conductor | ($mm^3$) |

The derivation for the amount of power needed to operate a coil begins with the basic definition of power.

$$P = I^2R \tag{15}$$

The resistance R is the resistance of the winding and can be written in the form of Eq. (16) where $\rho$ is the resistivity of the conductor, $L_w$ is the length of the wire, and $A_w$ is the area of the wire.

$$R = \rho\frac{L_w}{A_w} \tag{16}$$

Substituting Eq. (16) into Eq. (15) and using Eq. (13) to replace the current with the current density yields,

$$P = \frac{\rho I_d^2 A_c^2 L_w}{N^2 A_w} \tag{17}$$

The length of the wire can be written in terms of the conductor volume and packing factor, $\gamma$. The packing factor is a constant used to represent the ratio of the actual conducting wire volume to the volume allowed for the conductor. This is discussed in detail in the optimization section of this paper.

$$L_w = \frac{V_c}{\gamma A_w} \tag{18}$$

Substituting Eq. (18) into Eq. (17) yields,

$$P = \frac{\rho I_d^2 A_c^2 V_c}{\gamma N^2 A_w^2} \tag{19}$$

The number of turns N multiplied by the area of the wire $A_w$ is actually the area of the conductor $A_c$, making this substitution gives the final definition of the coil power consumption as,

$$P = \rho I_d^2 \frac{V_c}{\gamma} \tag{20}$$

## FORCE / POWER EQUATION

The force of a coil and the power consumption of a coil have now been defined. The final efficiency equation can now be defined simply by dividing the force equation, Eq. (14), by the power equation Eq. (20).

$$\frac{F}{P} = \frac{\mu_0 \gamma A_c^2 A_g}{8 L_g^2 \rho V_c} \tag{21}$$

## COIL DESIGN

In order to optimize the physical parameters of an electromagnet the electromagnetic force equations must be transformed into physical parameters. Starting with the **Eq. (21)**, the variables $V_c$, $A_c$, and $A_g$ must be transformed into physical quantities. The volume of the conductor $V_c$ is calculated as,

$$V_c = h\pi((r+c)^2-(r)^2) = hc\pi(c+2r) \tag{22}$$

The area of the conductor $A_c$ is defined as,

$$A_c = h \cdot c \tag{23}$$

The surface area of iron exposed to the gap must be defined at the center of the coil, $A_{gr}$, and at the outer iron wall of the coil, $A_{gw}$.

$$A_{gw} = \pi(r+c+t)^2-\pi(r+c)^2 = \pi(t^2+2t(r+c) \tag{24}$$

$$A_{gr} = \pi r^2 \tag{25}$$

Substituting the values of $V_c$, $A_c$, and $A_{gr}$ into **Eq. (21)** transforms the F/P equation into the physical parameters of the coil. (The reasons for substituting $A_{gr}$ instead of $(A_{gr}+A_{gw})$ will be discussed later.)

$$\frac{F}{P}(h,c,r,t) = \frac{\mu_0\gamma}{8\rho L_g^2}\frac{(hct(t+2(r+c))}{(2r+c)} \tag{26}$$

This one equation contains four unknowns (assuming the gap distance is given) which means that three more equations are needed in order to solve the system. Circuit theory states that the magnetic flux of the electromagnet is constant throughout the magnetic circuit. Since the iron saturation limit of the magnet is a constant, it can be inferred that the two exposed surface areas of the magnet must also be equal. This constrains the two values of $A_{gr}$ and $A_{gw}$ to be the same. By equating $A_{gr}$ and $A_{gw}$ a new constraint equation can be found.

$$t^2+2rt+2ct-r^2 = 0 \tag{27}$$

This leaves us with two equations and four unknowns. We therefore still need two more equations. These equations come from the constraints applied to the system. The first constraint equation restricts the magnitude of the magnetic flux density to keep it below the iron saturation value, nominally 2 Tesla for commercial grade iron. To keep the set of equations and the design of the coil general the maximum value of the flux density will be written as $B_{max}$.

$$B_{max} \geq \frac{\mu_0}{2}\frac{(NI)}{L_g} = \frac{\mu_0}{2}\frac{(I_d A_c)}{L_g} = \frac{\mu_0 I_d h c}{2L_g} \tag{28}$$

This equation adds a new unknown $I_d$. There is an equation for $I_d$ but it introduces unwanted variables into the equation set. In order to avoid this the new equation will be a constraint equation limiting the maximum value of the current density according to the material properties of the conductor material.

$$0 \le I_d \le I_{d_{max}} \tag{29}$$

The remaining constraint equation can be found by limiting the overall size of the coil assembly. If the volume of the coil is not constrained then the optimum coil volume will grow to infinity and the current density will drop towards zero. This equation will add the fifth equation to the set of five unknowns.

$$\frac{V}{\pi} = t^3+(h+2(r+c))t^2+(2h(r+c)+(r+c)^2)t+h(r+c)^2 \tag{30}$$

The equations can now be grouped into a solution set. The solution set contains five equations and five unknowns. This would appear to be enough equations to solve for the optimum coil geometry but it is not. The given set of equations will optimize the F/P equation but it will do so in the wrong "direction." The set of equations follow a gradient that leads the optimum solution to zero force and zero power. In order to avoid this a sixth equation must be added to the solution set. This equation will force a finite force output from the coil.

$$F_{min} = \frac{\mu_0 I_d^2 A_C^2 A_g}{8L_g^2} = \frac{\pi \mu_0 I_d^2 h^2 c^2 r^2}{8L_g^2} \tag{31}$$

This leads to the total solution set.

This leads to the total solution set.

Summary for Force/Power equation set:

$$\frac{F}{P}(h,c,r,t) = \frac{\mu_0 \gamma}{8\rho L_g^2}\frac{(hct(t+2(r+c))}{(2r+c)}$$

$$t^2+2rt+2ct-r^2 = 0$$

$$B_{FE_{max}}(h,c,I_d) \geq (\frac{\mu_0 I_d}{2L_g})hc$$

$$F_{B_{min}}(h,c,r,I_d) = (\frac{\pi\mu_0}{8L_g^2})h^2c^2r^2I_d^2$$

$$\frac{V(r,c,h,t)}{\pi} = t^3 + (h+2(r+c))t^2 + (2h(r+c)+(r+c)^2)t + h(r+c)^2$$

$$0 \leq I_d \leq I_{d_{max}}$$

(32)

Eq. (27) can be reduced to a quadratic in t. Solving the quadratic results in t being a function of r and c.

$$t(r,c) = -(r + c) + \sqrt{(r + c)^2 + r^2} \quad (33)$$

The new formulation for t(r,c) can be substituted into Eq. (21) to obtain F/P as a function of only h, c, and r. The same solution can be found by substituting $A_{gw}$ into Eq. (21).

substitute t(r,c) into the solution of V but this does not result in a very usable form. The equation can be simplified using one of the constraints. Looking back at the original derivation of V and the fact that $A_{gr}$ equals $A_{gw}$ it is possible to develop a relation for V without a cubic t involved. Instead of defining the outer radius as (r+c+t) and multiplying its square by (h+t) the surface area can be written as a sum of the inner and outer volumes. From Eq. (24) and Eq. (25) it is known that the outer area is equal to $\pi r^2$. Therefore the total volume can be written as the total height of the coil multiplied by $\pi(r+c)^2+ \pi r^2$. Then the value of t can be easily substituted into the new volume equation.

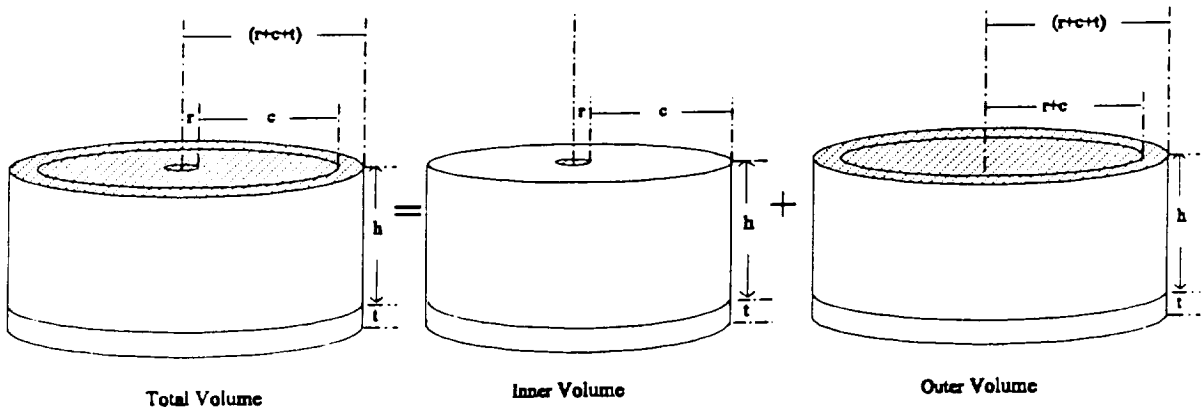


**Figure 3: Constraint defined coil volume**

The set of equations has now been reduced to a set of five equations and five unknowns.

$$\frac{V(r,c,h)}{\pi} = ((r+c)^2+r^2)(h-r-c+\sqrt{(r+c)^2+r^2}) \qquad (35)$$

The total solution set containing all the optimizing equations and constraint equations are summarized in Eq. (36a-e) and Eq. (37).

$$\frac{V(r,c,h)}{\pi} = ((r+c)^2+r^2)(h-r-c+\sqrt{(r+c)^2+r^2}\ ) \tag{35}$$

The total solution set containing all the optimizing equations and constraint equations are summarized in Eq. (36a-e) and Eq. (37).

$$(a) \quad \frac{F}{P}(r,h,c) = (\frac{\mu_0 \gamma}{8\rho L_g^2})\frac{r^2 hc}{2r+c}$$

$$(b) \quad B_{\max}(h,c,I_d) \geq (\frac{\mu_0}{2L_g})hcI_d$$

$$(c) \quad F_{\min}(h,c,r,I_d) = (\frac{\pi\mu_0}{8L_g^2})h^2c^2r^2I_d^2 \tag{36}$$

$$(d) \quad \frac{V(r,h,c)}{\pi} = ((r+c)^2+r^2)(h-r-c+\sqrt{(r+c)^2+r^2}\ )$$

$$(e) \quad 0 \leq I_d \leq I_{d_{\max}}$$

$$t(r,c) = -(r + c) + \sqrt{(r + c)^2 + r^2} \tag{37}$$

Summary for Force/Power equation set:The t(r,c) equation will still be needed to determine t after the optimal values of r and c have been found. It has been separated from the other equations as a reminder that it has already by substituted into the other equations.

## COIL OPTIMIZATION

The coil was optimized using a commercial version of MATLAB. The optimization code used the Sequential Quadratic Programming method to optimize the equations. The basic optimization codes were supplemented with additional codes needed for this application.

The equation set defined in Eqs. (36) & (37) requires that the optimization take place over a range of forces, a range of gap distances, and a range of coil volumes. Because of this some additional MATLAB codes to control the optimization processes were needed. These codes optimized a coil of a set volume over a gap distance ranging from 0.2 mm to 15 mm in 0.2mm increments. The force limitations were prescribed for each gap distance and ranged from 0 N to the maximum force a coil of that volume could produce. Since this maximum force was different for each coil volume the force increment was simply the maximum force divided by 80 steps. Five coil volumes were optimized. The original volume was chosen to be 120 $in^3$ ($1.93x10^6$ $mm^3$). The other four volumes were equal to 50%, 75%, 125%, and 150% of 120 $in^3$. To keep the programs general, the maximum force per coil volume was found through a similar optimization process using many of the equations derived in this paper. These results are shown if Fig. 5. In order to get results that could be compared to known cases commercially standard materials were modelled. The conductor was chosen to be copper and the core material was chosen to be iron.

The variations in coil performance due to different construction methods was handled by choosing the best possible design. When the conducting wire is wrapped inside a coil it is not possible to fill all the volume with conductor. This is because of the wire geometry and the fact that each wire is surrounded by a thin layer of insulation, as shown in Fig. 6. When actual

coil calculations are being made this conductor geometry and winding style is known and can be accounted for using a packing factor $\gamma$. This factor can range from 0.5 for poorly wound round conductor to 0.95 for tightly wound square conductor. For the actual optimization the packing factor was defined as 1. While this is not actually a feasible value it does not affect the trends.

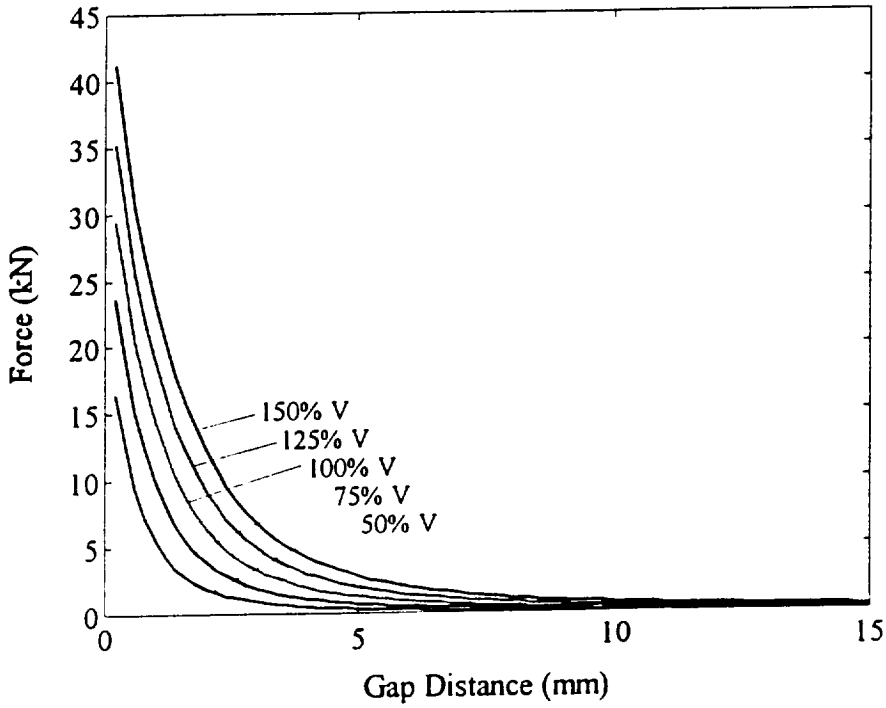


**Figure 4: Maximum force per volume optimization results**

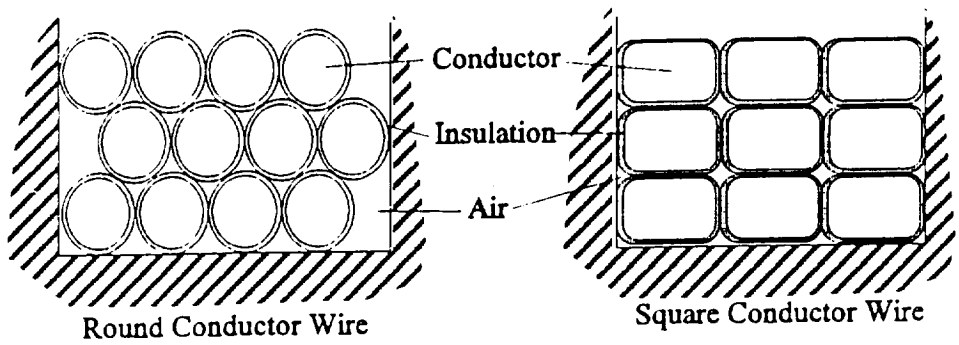


**Figure 5: Conductor winding methods**

## OPTIMIZATION RESULTS

The final optimization results show that the coil geometry remains constant as the gap distance changes. This allows for the individual geometry components to be compared over the range of forces and volumes. The optimization result for the core radius, r, is shown in Fig. 6. The variable r physically represents the surface area of the iron as $\pi r^2$. Plotting this surface area against force shows the linear relationship in Fig. 7 which agrees with Eq. (2). Mathematically this results in two more equations that represent an optimum coil design. Fig. 6 shows that the coil radius is solely a function of force and independent of gap distance and volume, this leads to Eq. (38). The

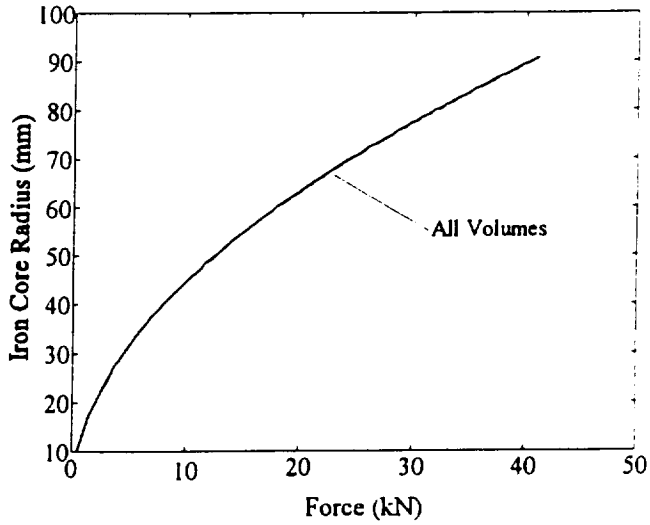


**Figure 6: Optimization results for core radius**

$$r(F) = \left(\frac{2\mu_0}{\pi B_{max}^2}\right)^{1/2} F^{1/2} \quad (38)$$

constant slope of the area plot can be equated to the magnetic flux density, resulting in Eq. (39) This is important because it shows that for a properly

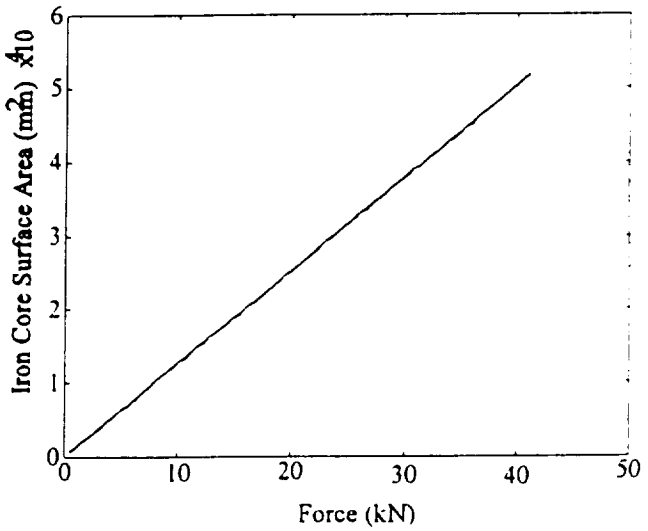


**Figure 7: Optimization results for iron surface area.**

$$\frac{2B_{max}}{\mu_0} = \frac{hcI_d}{L_g} = C_1 \tag{39}$$

designed coil the magnetic flux density and field intensity will remain constant at it's maximum allowable value. The equation itself only shows B to be a constant, the optimization results show it to be at its maximum value. The equation also shows that since the conductor depth and height remain constant as the gap changes the current density varies directly with gap distance. This result is shown in Fig. 8 and makes it possible to graph the 3-D results for power consumption and force per unit power in a 2-D format. These graph are plotted in Fig. 9 and Fig. 10. Because these plots are plotted in a 2-D format instead of a 3-D format it is now clear to see how the force efficiency varies with volume size. Fig. 9 shows that the power requirement per volume needed to achieve a particular force output. Fig. 10 shows the force per power ratio for the different volumes. The larger the volumes the more efficient the coil at delivering the required force output. This raises the question of wether or not there is an optimum coil volume for a designated force and gap distance. The initial optimization results show that the answer to this question is no. The efficiency of the five

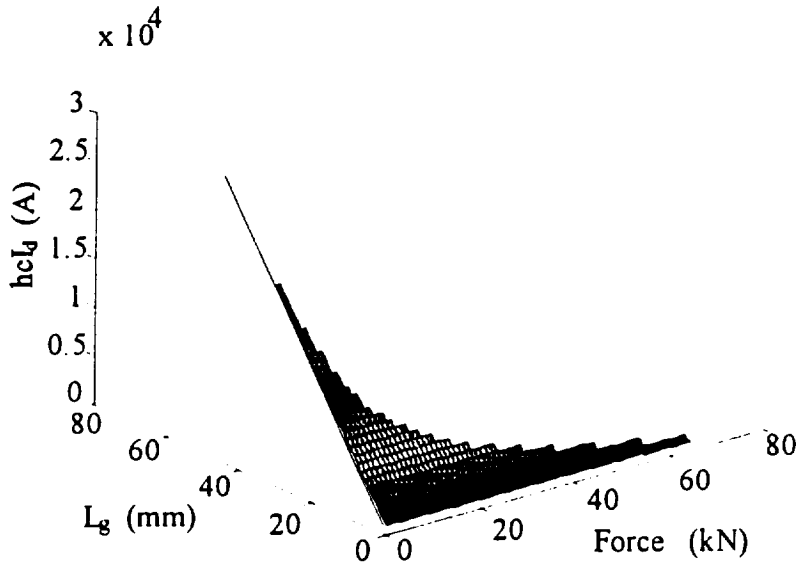


**Figure 8: Product of $hcI_d$ vs force and gap distance**

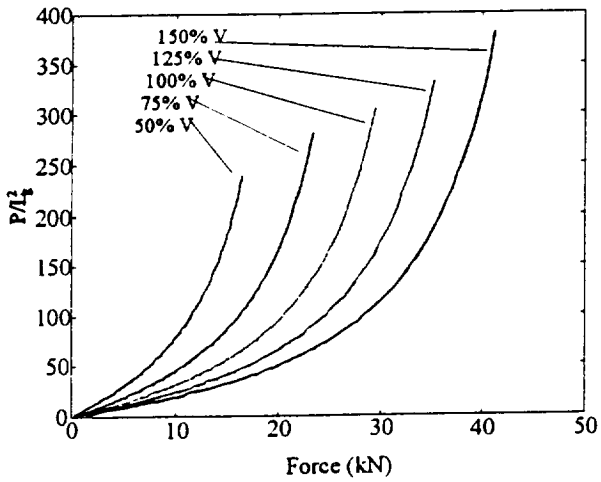


**Figure 9: Optimization results for $P/L_g^2$**

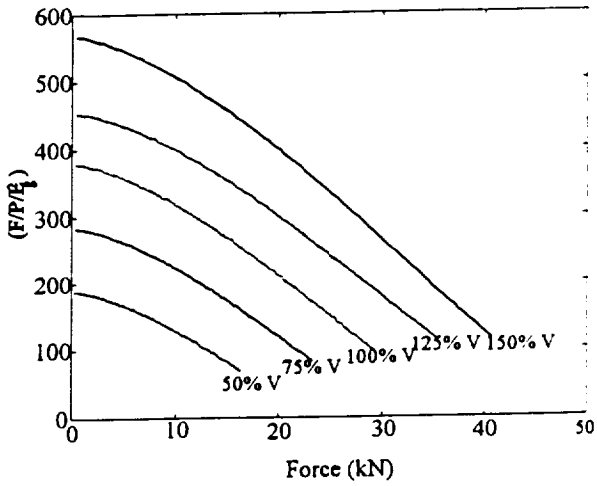


**Figure 10: Optimization results for $F/P/L_g^2$**

volumes are compared to five different force values in Fig. 11. The result appears to be a linear increase in efficiency with an increase in volume. This suggests that the coil efficiency will continue to increase as the volume grows infinitely large. This may not always be the case. The range of volumes compared here is a small range. In order to make a more definite conclusion more cases would have to be run with much larger volumes.

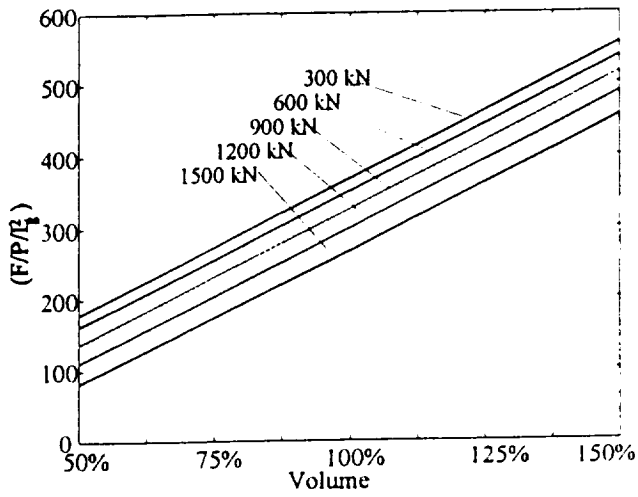


**Figure 11: Optimization results for coil efficiency vs. volume**

One of the questions at the beginning of this study was how the general shape of the coil varied with efficiency. There were three distinct geometries that were at question. The first was the radius of the iron core which was discussed earlier. The

remaining two were the coils aspect ratio and the ratio of the conductor height to conductor width. The aspect ratio is plotted against force per power efficiency in Fig. 12. These results show that the tall, thin coil is more efficient then a short, fat coil. The ratio of conductor cross

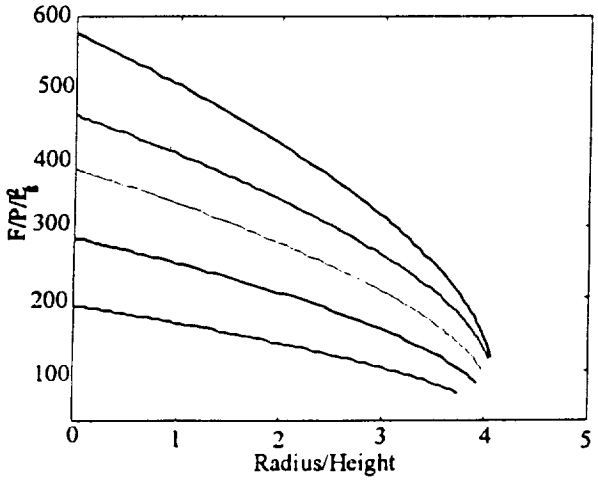


**Figure 12: Optimization results of efficiency vs. aspect ratio**

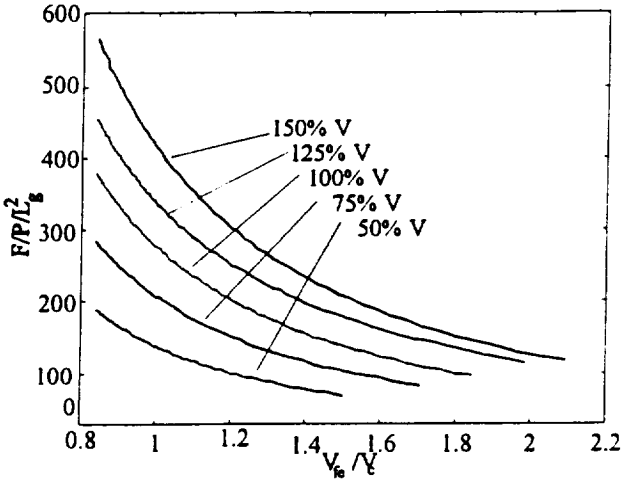


**Figure 13: Optimization results for coil efficiency vs. volume ratio**

sectional height to cross sectional depth shows the same behaviour in Fig. 14. This result makes sense because a tall coil will allow a small core radius and a large conductor volume.

This large conductor volume means that the current density can have a small value while still providing the necessary force output. As the coil flattens out more of the volume is consumed by the core and wall so the volume

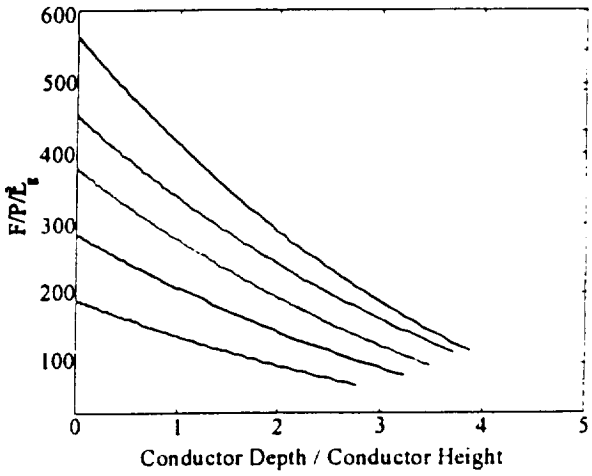


**Figure 14: Optimization results of efficiency vs. conductor cross section aspect ratio**

of the conductor must grow smaller. In order to produce the maximum magnetic flux density the current density must increase. This increase causes the power requirements to increase as the square of the current density. The volume ratio is plotted against the coil efficiency in Fig. 13.

The next important result comes from the fact that minimum current density leads to minimum power. Eq. (36b) shows that the product of conductor depth, conductor height, and current density for a given gap distance remains constant. Minimizing the current density in Eq. (36b) maximizes the conductor area. The optimization results for conductor cross sectional area are compared to the coil efficiency in Fig. 15 and show the same conclusion. This behaviour is very important because it identifies the controlling aspects of the coil.

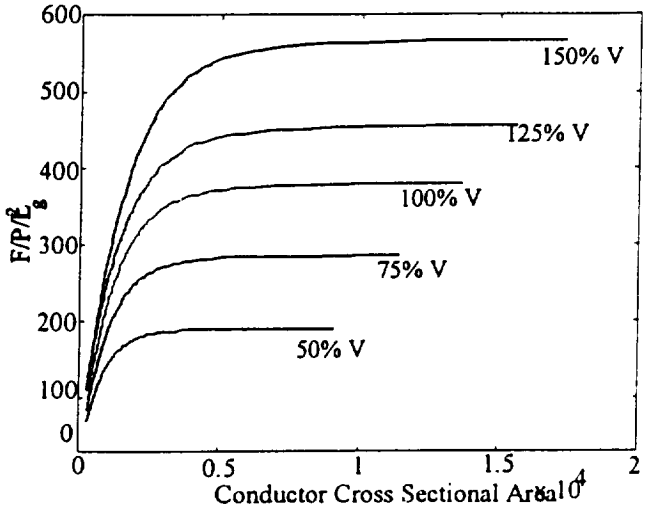


**Figure 15: Optimization of conductor area vs. coil efficiency**

The optimum radius of the core of the electromagnet is found from Eq. (38). The radius constrains the thickness of the coil wall and the total volume of the coil is defined. That leaves a constrained value of cross sectional coil area. It is also known that this coil area should be as tall and narrow as possible to obtain the largest amount of force per power. The general optimized geometry of a radially symmetric electromagnet has now been defined.

The trends in the remainder of the geometric variables do not offer any new insights into the controlling factors of the coil efficiency but are important to the actual coil design. These results are shown in Fig.s 16, 17, 18, and 19.

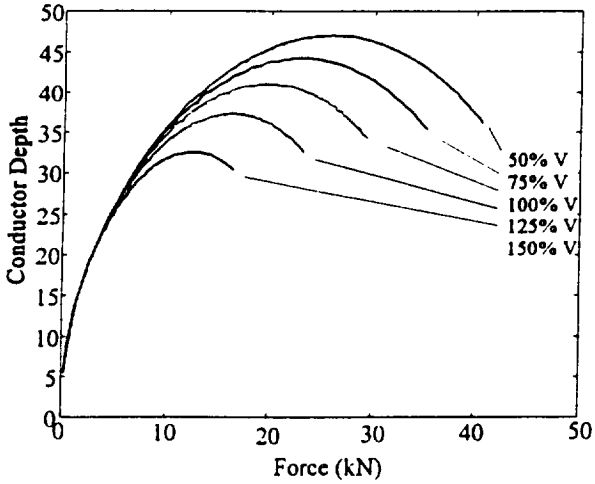


**Figure 16: Optimization results for conductor depth**

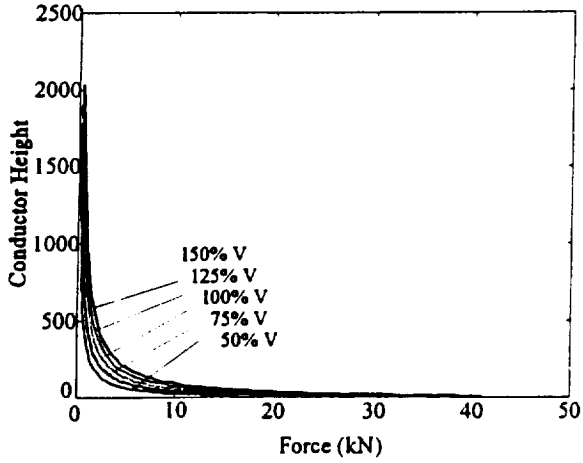


**Figure 17: Optimization results for conductor height.**

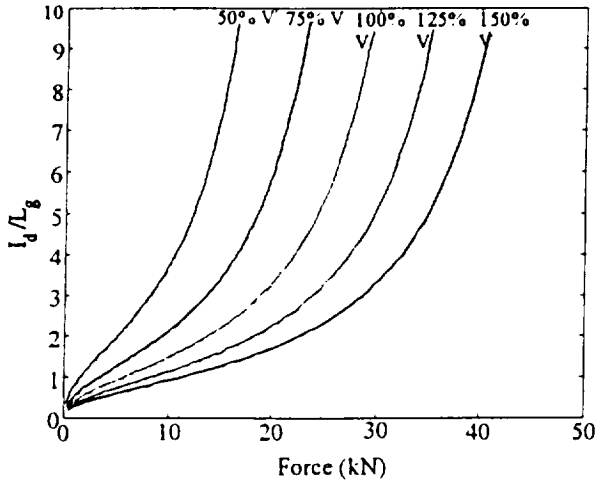


**Figure 18: Optimization results for $I_d/L_g$**

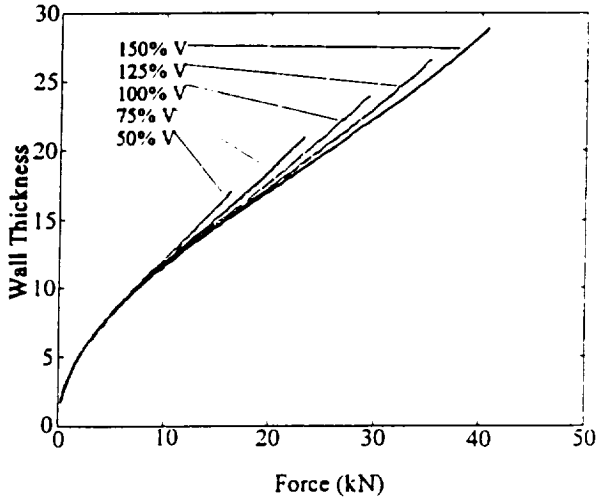


**Figure 19: Optimization results wall thickness**

## CONCLUSIONS

A radially symmetric iron-cored electromagnet being designed for maximum force per power should be designed with certain characteristics in mind. The application for which the coil is being designed should provide the designer with a specific force output or range of force outputs, the nominal air gap or range of gap distances, and an allowable coil volume. Having these pieces of information the coil can be optimized for efficiency. The larger the volume of the coil the higher its efficiency. The coil should be designed to operate at it's maximum allowable magnetic flux density. The magnetic flux density limit is controlled by the material used to construct the magnet, therefore a material with a high saturation limit allows for the best design. The core of the electromagnet should have a radius indicated by the equation,

$$r(F) = \left(\frac{2\mu_0}{\pi B_{max}^2}\right)^{1/2} F^{1/2}$$

Once the radius of the core has been determined the conductor volume should be optimized and maximized. The conductor volume should be made as large as possible and as tall and thin as possible. This volume is limited by the wall thickness constraint in Eq. (37). The optimum values for these geometries can be backed out of Eq.s (36d) and (37).

Further studies are planned for both small and large gap systems. The small gap research will continue on with non-symmetric coil designs. The geometries will be allowed to vary in both the radial direction and in height. These results will aid in the large gap system optimization process which will follow a similar path as the small gap optimization process. The final

results should lead to the most efficient electromagnet designs possible. While the results will be immediately applicable to existing magnetic systems the long term goal of this study is to increase the applicability of new magnetic technologies for use in the aerospace industry.

## REFERENCES

1. Ida, N. and Bastos J., Electromagnetics and Calculation of fields, Springer-Verlag, 1992.

Appendix B

Britcher, C.P.: Provision of support interference free static and dynamic test capability in high Reynolds number facilities. Presented at the Workshop on Needs for High Reynolds Number Facilities to Design the Next Generation of Sea and Air Vehicles, Arlington, VA, June 1997.

Needs for High Reynolds Number Facilitites to Design the Next Generation of Sea and Air Vehicles
Arlington Hilton, Arlington, VA, June 18-19, 1997

# Provision of Support-Interference-Free Static and Dynamic Test Capability

Colin P. Britcher
Department of Aerospace Engineering
Old Dominion University
Norfolk, VA

Acknowledgements : This work has been partially supported by NASA Langley Research Center under various Grants and currently under Cooperative Agreement NCC-1-248, Technical Monitor Nelson J. Groom

## Why Do We Need Interference-Free Static and Dynamic Test Capability?

A variety of fundamental limitations continue to bedevil wind tunnel testing :

- (Low) Reynolds numbers
- Support interference
- (Inadequate) dynamic simulation
- Wall interference
- (Poor) flow quality
- (Lack of) high enthalpy flows

Low temperature and/or high pressure tunnels can provide high Reynolds numbers; Wall interferences can be assessed and corrected (a far-field effect); Flow quality issues are under study; High h's are beyond current scope; Support interference corrections are fundamentally very difficult (a near-field effect); Dynamic simulation requires the ability to generate complex trajectories at relatively high dimensionless frequencies (mechanically difficult).

## How Do We Achieve ..... ?

Magnetic Suspension and Balance Systems (MSBS) have the potential to completely eliminate support interference and provide new dynamic capability.

## Technical Background

The wind tunnel test section is surrounded by electromagnets

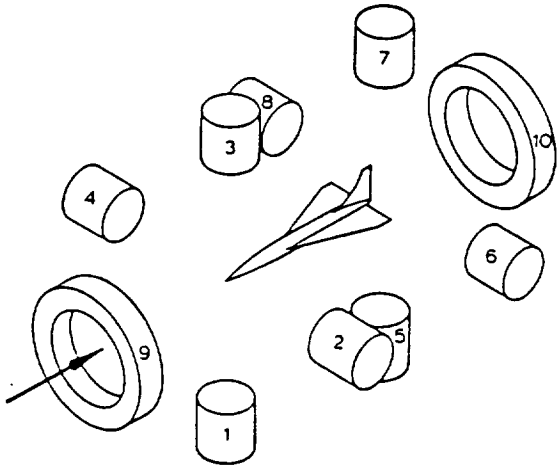


Whole body forces and moments are obtained by E/M current calibration

Stability is maintained by a feedback control system

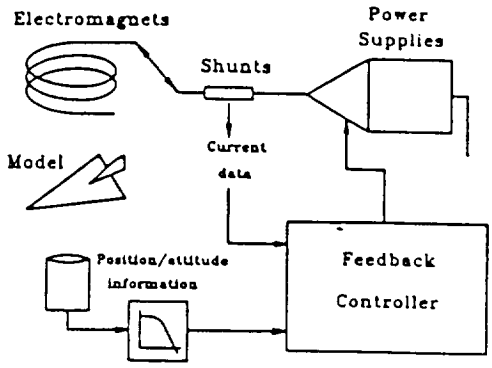


Dynamic capability is inherently provided with a feedback controller

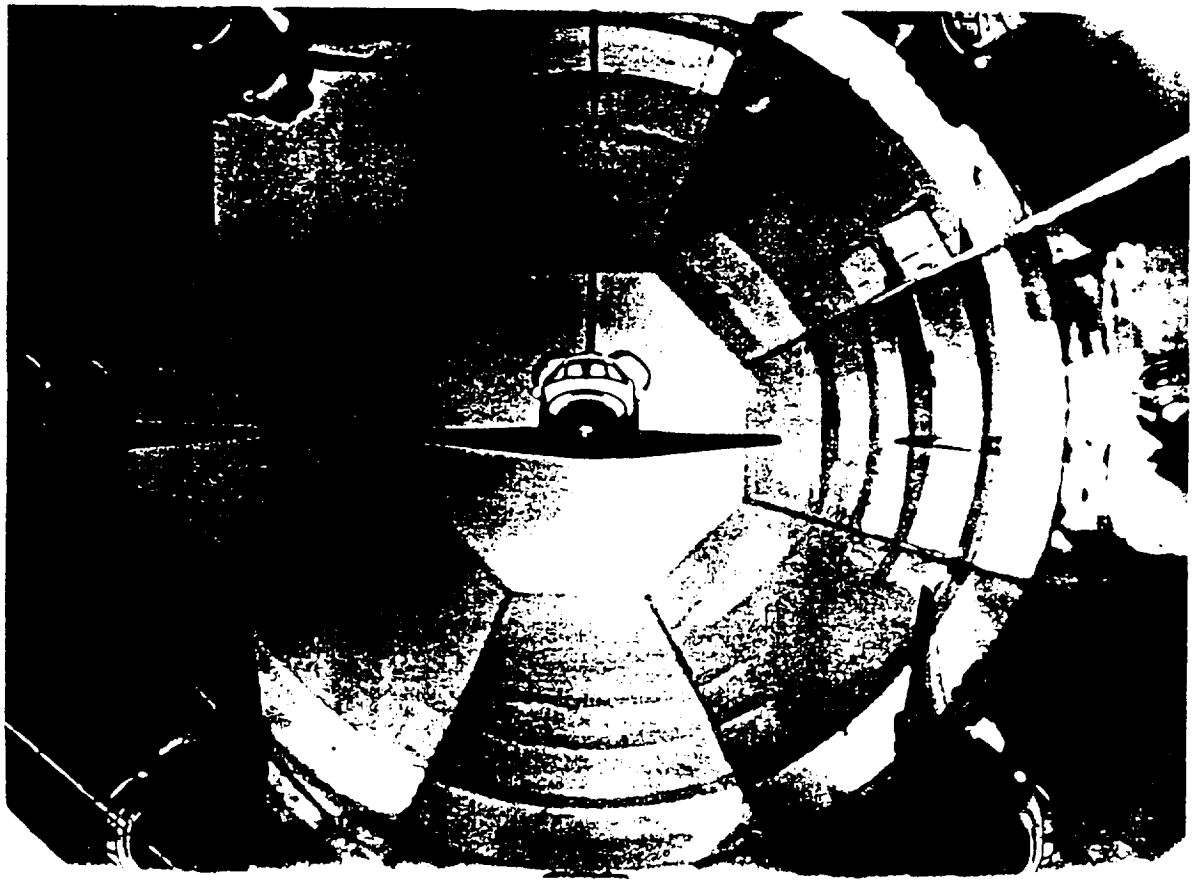

## Why is MSBS not a "Production" Technique ? (a little history)

- Wind tunnel MSBSs have been around for 40 years (ONERA, 1957)
- More than 20 systems have been built, in 7 different countries
- Test Mach numbers have ranged from subsonic to hypersonic
- Testing includes static force/moment, support interference & dynamic stability
- The largest system yet constructed is for a 60 cm ( $\approx$ 2 foot) test section
- Design studies in the 1980's concluded that a system for a large, high Reynolds number transonic wind tunnel was technically feasible, albeit rather expensive (G.E. and M.M.I.). $\Rightarrow$ *U.S. MSBS work was curtailed.*
- At least 5 countries have currently active research and development efforts
- Applications currently under study include : Ultra-high Reynolds numbers High angle-of-attack aerodynamics; Transonic, cryogenic wind tunnel;

**Numerous technical developments over the last decade have greatly enhanced the technical feasibility and potential capability of MSBSs.**

NASA
L-85-3826

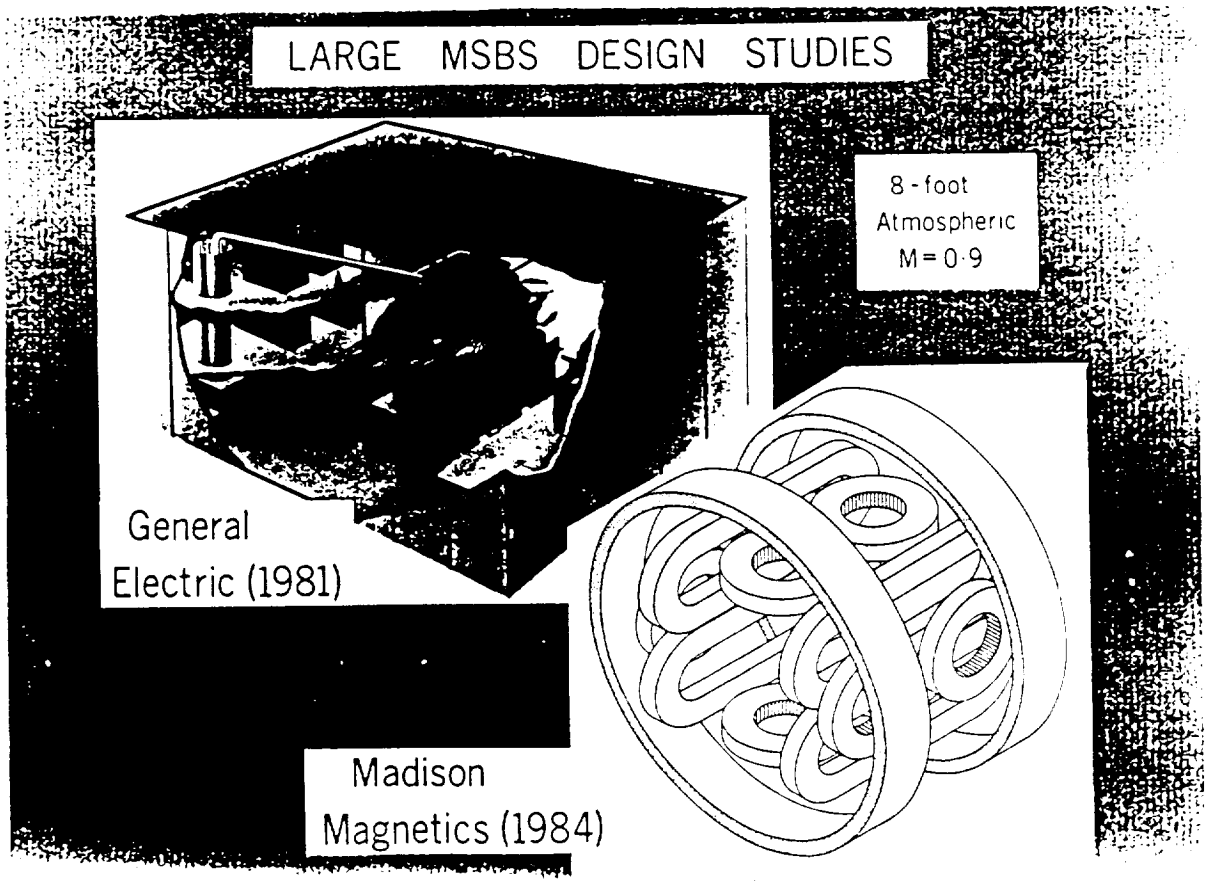

## Currently Active MSBS R&D Programs

| Organization | Size | Current Application | Current Status |
|---|---|---|---|
| Old Dominion University[1] | 6-inch | System R&D | Recommissioning |
| Oxford University[2] | 3-inch | Hypersonic aerodynamics | Active |
| NAL, Japan | 4-inch | System R&D | Active |
| NAL, Japan | 23-inch | System R&D | Active |
| NCKU, Taiwan | 6-inch | System R&D | Active |
| CIT/CARDC, China | 6-inch | System R&D | Active |
| NASA Langley Research Center | 13-inch | Low-speed, R&D | Inactive |
| MAI / TsAGI, Moscow | 18-inch | System R&D | Inactive |

The National High Magnetic Fields Laboratory (NHMFL) is also engaged in design studies for the ultra-high Reynolds number application.

1 - Formerly NASA / MIT system  2 - Arguably the only current "production" facility

## Current U.S. Systems (c. 1997)

NASA LaRC "13-inch" MSBS

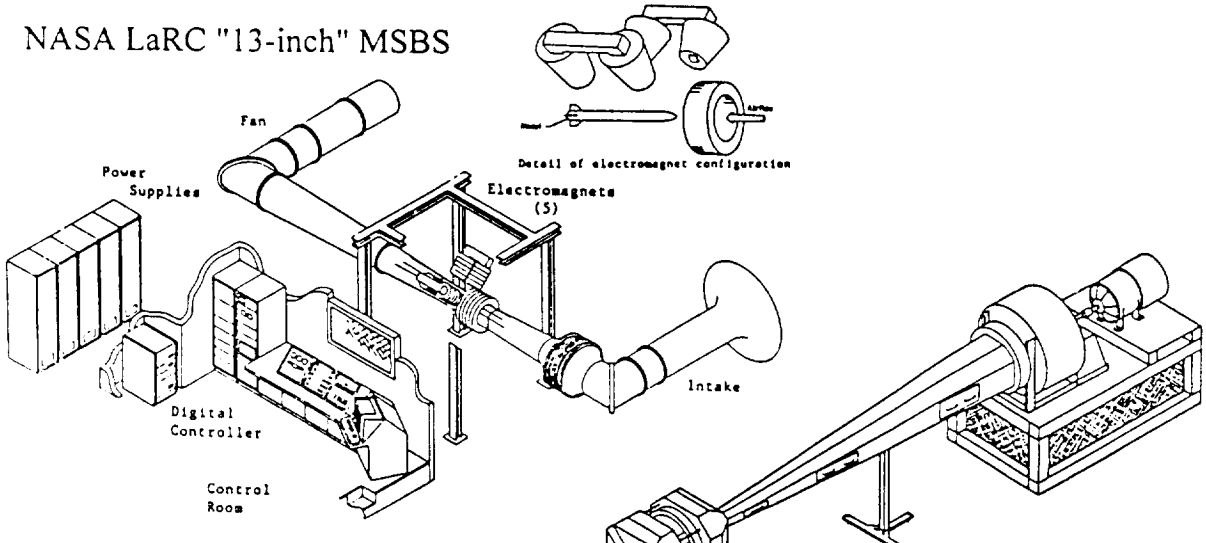


ODU (ex-NASA/MIT)
"6-inch" MSBS

## NHMFL Passive MSBS Design

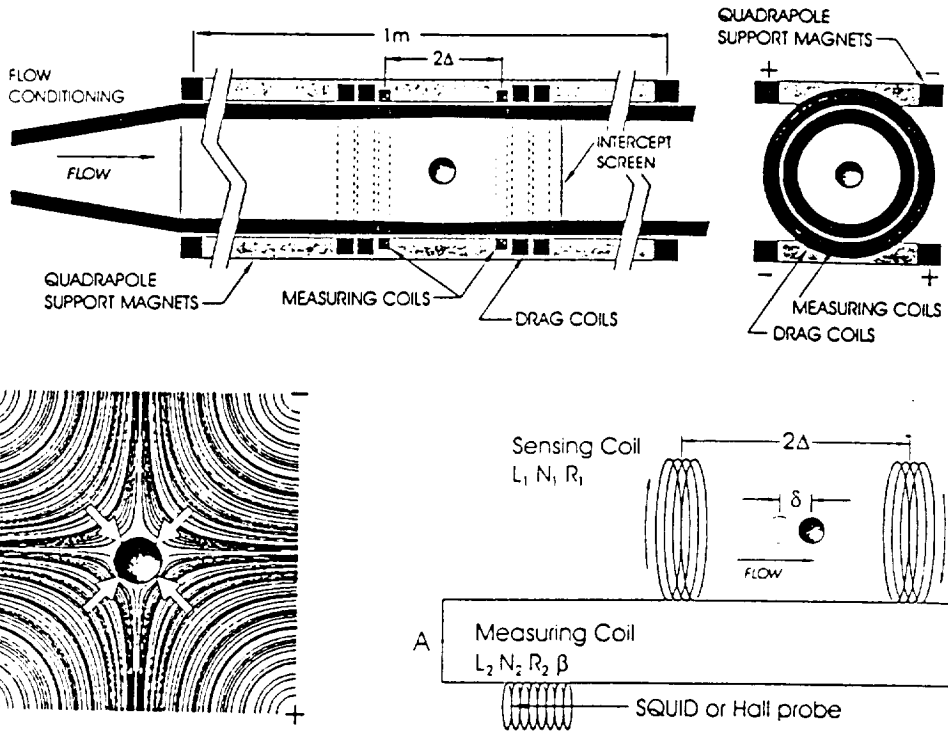


## Technical Developments - Particularly Over the Last Decade

- Elimination of support interference; relatively simple provision of extreme attitudes (90° pitch, sideslip etc.) and provision of more-or-less arbitrary model motions have all been demonstrated in small-scale MSBSs
- A new magnetic configuration (tranversely magnetized cores) has been demonstrated at small scale. Potentially solves the "roll control" problem
- New permanent magnet materials - Neodymium-iron-boron (NdFeBo) in the last decade; doped acicular iron powder within the last 1-2 years
- High Temperature Superconductors (HTS) continue rapid advances - practical prototypes for engineering applications are emerging - the first large-scale commercial devices shipped in 1997 (high $T_c$ transformers)
- Advanced control approaches (LQR/LQG, fuzzy logic, etc.) have been applied to large-gap magnetic suspensions
- Systematic electromagnet configuration design methods under development - combine optimization codes with electromagnetic and control theory

## Support Interference - A Serious Problem in Static and Dynamic Tests

LaRC 13-inch MSBS results show up to 200% drag corrections to sting-on data !

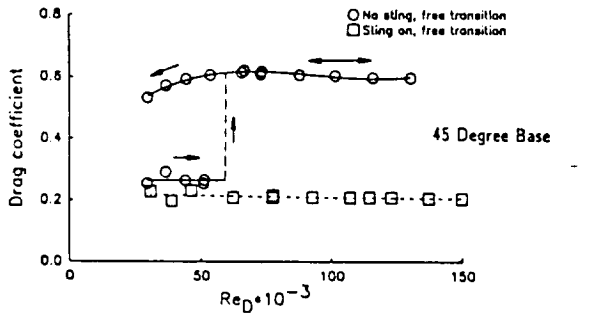


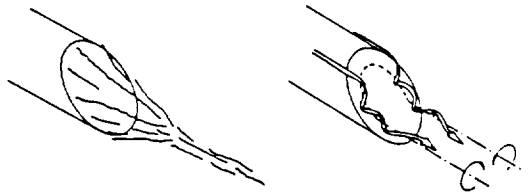


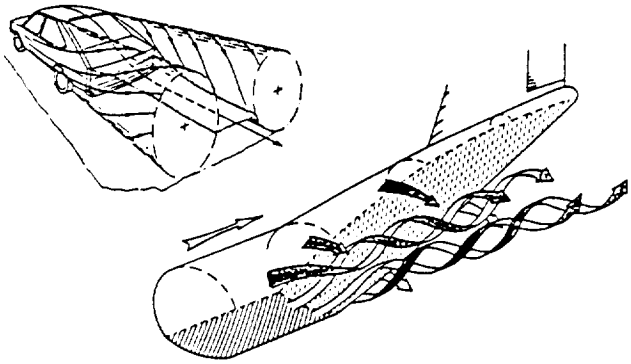

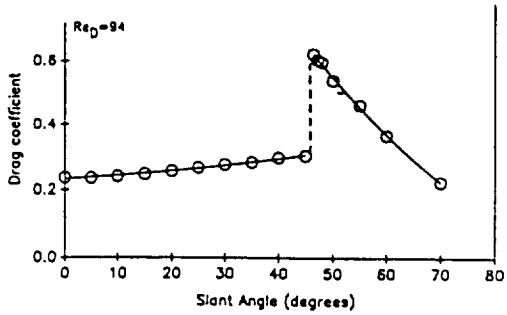


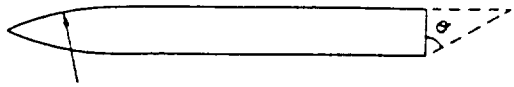

Typical dynamic test rigs (NAE and ARA shown) require massive support struts

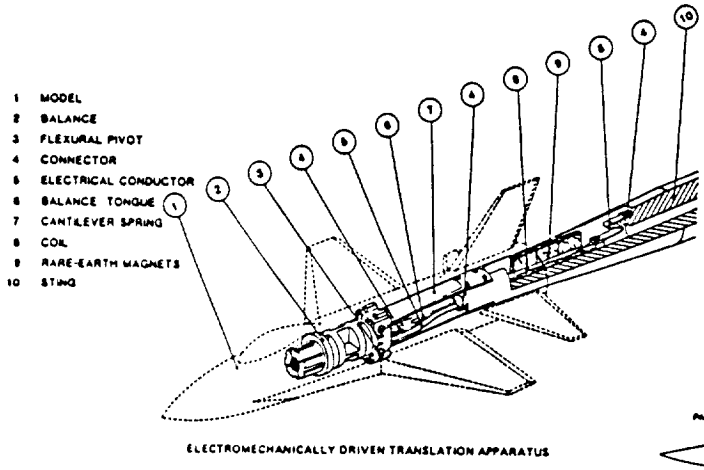


ELECTROMECHANICALLY DRIVEN TRANSLATION APPARATUS

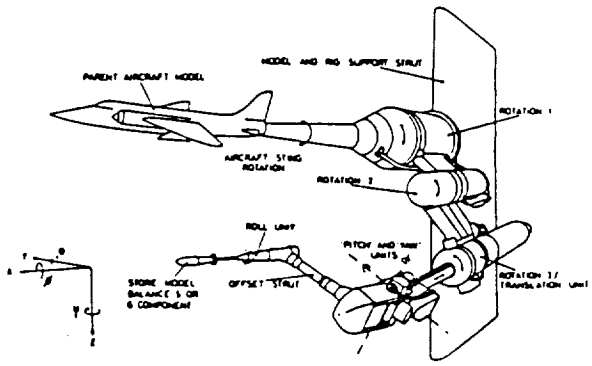

Reprinted from THE WALL STREET JOURNAL.
WEDNESDAY, MARCH 12, 1997


THE WALL STREET JOURNAL.
TEXAS JOURNAL

# American Superconductor to Announce Start of Transformer Project in Geneva

By Ross Kerber
*Staff Reporter of* The Wall Street Journal

WESTBOROUGH, Mass. – American Superconductor Corp. executives said they expect to announce today that an electric transformer for which the company supplied metal-ceramic composite wire has entered service in Geneva.

The project marks a major step in the company's attempts to commercialize its products for the electric power industry, American Superconductor President and Chief Executive Greg Yurek said in an interview.

The demonstration transformer, developed by a unit of ABB Asea Brown Boveri Ltd. and several European government partners for about $5 million, is part of a substation that supplies electricity to the headquarters of Geneva's municipal utility.

American Superconductor develops components to make the generation, transmission and consumption of electricity more efficient, and Mr. Yurek said he expects utilities and power consumers will find increasing benefits from investing in such technologies as the electric industry is restructured to become more competitive. Using superconductive transmission cables, utilities will be able to carry more electricity along the same rights-of-way, he said, while factories and other large consumers will be able to cut their power consumption by installing motors based on the same wires.

## Difficult Research

"The [superconductive] wire will be adopted for the same reasons that fiber-optic components became popular" as the telephone industry was deregulated, he said. "In both cases, the advanced wires let you move more of the commodity."

The superconductive properties of some ceramics have been difficult for researchers to tap for commercial applications because of the brittleness of the material. To solve that problem, American Superconductor manufactures a composite material by combining ceramics with metals such as silver alloys, allowing the ceramics to be wrapped into coils for commercial sales.

The company is still years away from offering the products it will need to become profitable, however. Mr. Yurek said he couldn't discuss target dates for profitability, but said the company's goal is to provide the components needed for ABB to offer commercial transformers for sale by 2001, "give or take six months." The company also has partnerships to develop wire for motors and power transmission applications. For the fiscal third quarter ended Dec. 31, 1996, American Superconductor reported a loss of $1.7 million, or 18 cents a share, compared with a loss of $2.5 million, or 26 cents a share, a year earlier. Revenue increased 85% to $2.4 million from $1.3 million.

## Lighter, More Expensive

In Geneva, the transformer scheduled to enter service will use American Superconductor's high-temperature wire, which doesn't need expensive and bulky cooling components. Future, larger generations of superconductive transformers will weigh roughly half as much as traditional transformers using copper coils, allowing utilities to install smaller power substations with increased capacity. The equipment will be 50% to 75% more expensive than conventional transformers, Mr. Yurek said, but that will be offset by savings in maintenance costs.

Transformers are used to regulate the voltage of power. The wire also eliminates the need to surround the power-transforming coils with insulating oil, which is prone to leakage and fires.

In addition to the partnership with ABB, American Superconductor supplies wire for motors through a partnership with Rockwell Corp.'s Reliance Electric unit, and supplies wire for transmission cables through a partnership with Pirelli Cavi SpA.



## Tranverse Magnetization Configuration

$$\vec{F}_c \approx \forall \left(\vec{M}.\nabla \vec{B}_o\right) \; ; \; \vec{T}_c \approx \forall \left(\vec{M} \times \vec{B}_o\right) \; ; \; \vec{T}_i \approx \forall \int_{\forall} \vec{M}_j \left\{\frac{\partial B_j}{\partial k}\right\} d\forall$$

With changes in orientation of magnetic core relative to electromagnet array :

$$\vec{\vec{F}}_c \approx \forall \left[T_m\right]\left[\partial B\right]\left[T_m\right]^{-1}\vec{\vec{M}} \; ; \; \vec{\vec{T}}_c \approx \forall \vec{\vec{M}} \times \left[\left[T_m\right]\vec{B}\right] \; ; \; etc.$$

This is already demonstrated with the 6 degree-of-freedom LAMSTF experiment

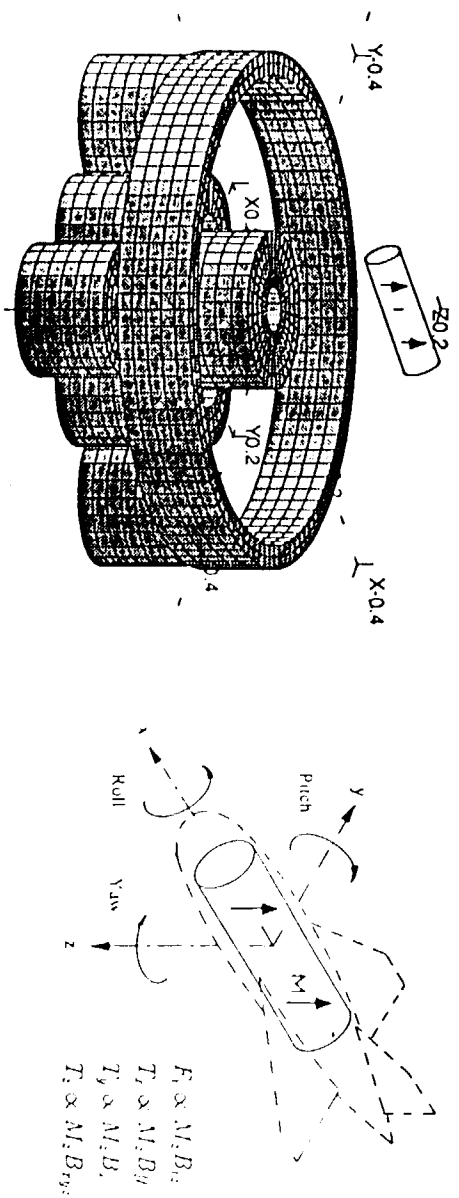

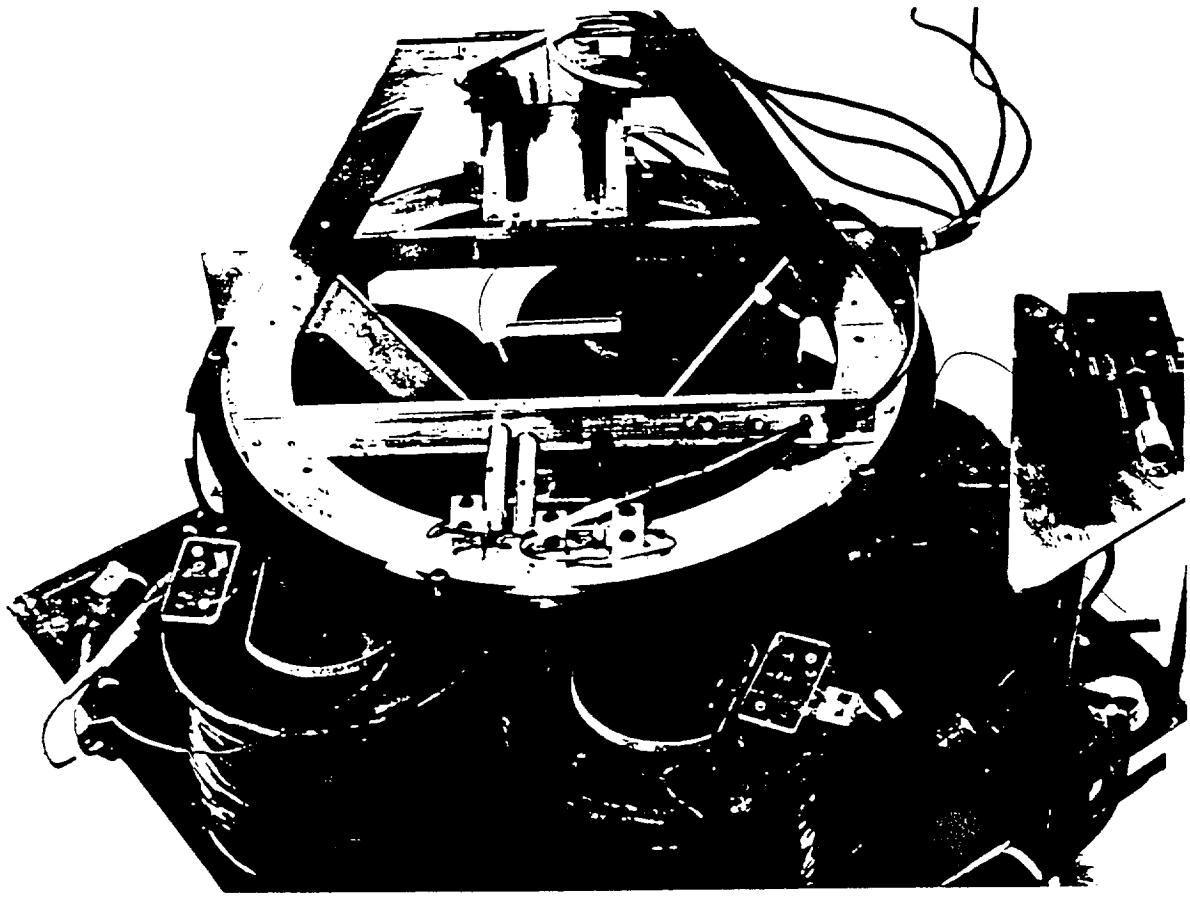

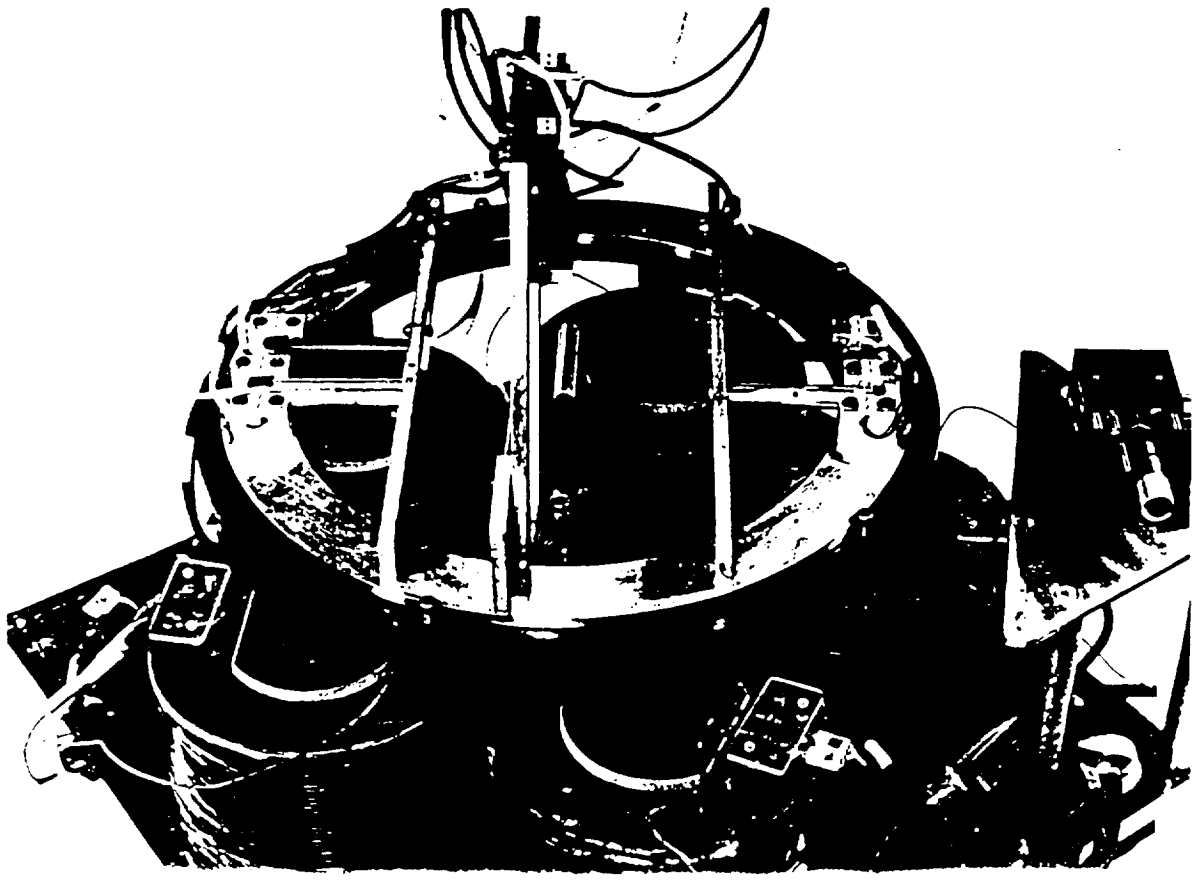

## Liquid and Gaseous Helium Facilities

- Relatively easy to achieve very high Reynold's numbers in low-speed flows
- Target length Reynolds number $10^9$, on slender, near-axisymmetric shape
  - data below derived from results of Oregon Workshop, Donnelly et.al.

| | Gaseous Helium | Helium I | Helium II |
|---|---|---|---|
| Temperature, K | 5.3 | 2.8 | 1.6 |
| Velocity, m/s | 40 | 10 | 4 |
| Unit Reynolds No., $m^{-1}$ | $3 \times 10^8$ | $3.8 \times 10^8$ | $4.4 \times 10^8$ |
| Dynamic pressure, Pa | 8725 | 7150 | 1160 |
| Model length, m | 3.3 | 2.63 | 2.27 |
| Test section size, m | 0.94 square | 0.75 square | 0.65 square |
| Max. model weight, N | 8700 | 4400 | 2830 |
| Drag force, N | 74.6 | 38.9 | 4.7 |

$\Rightarrow$ The application is quite benign from the perspective of forces and moments.

## Ultra-High Pressure Air Facility

- Very high Reynold's numbers, with acceptable dynamic pressures, can be achieved in low-speed flows with extremely high operating pressures
- Some preliminary work carried out by Smits et. al., Princeton University, where an ultra-high Reynold's number pipe flow facility already exists

| | Gaseous Helium | High Pressure |
|---|---|---|
| Temperature, K / Pressure, atm. | 5.3 K / 1 atm. | 288 K / 100 atm. |
| Velocity, m/s | 40 | 48.5 |
| Unit Reynolds No., $m^{-1}$ | $3 \times 10^8$ | $3.3 \times 10^8$ |
| Dynamic pressure, Pa | 8725 | 288,000 |
| Model length, m | 3.3 | 3.0 |
| Test section size, m | 0.94 square | 0.85 square |
| Max. model weight, N | 8700 | 7190 |
| Drag force, N | 74.6 | 2992 |

The application is within current technology in terms of size & forces/moments

## Opinions and Observations

- Wind tunnel MSBS is a technology that is too valuable to overlook or abandon
  ⇒ support interference elimination, improved capability for testing at extreme attitudes, unsteady aerodynamics and dynamic stability
- Technology continues to advance in many important areas, promising improved system performance and reduced cost
- Large systems for large, high-q tunnels will always be somewhat expensive
- The high Reynolds number application can be within current technology
- High Reynolds number tunnel designs must incorporate MSBS requirements
- Continued MSBS research is needed and worthwhile; can be synergistic with other programs - Maglev trains, electromagnetic launch, space payload pointing and vibration isolation, magnetic bearings, etc.
- Increased focus on unsteady aero. / dynamic stability has been proposed
- U.S. MSBS work has been at a low level, but critical skills still exist

Annular Momentum Control Device

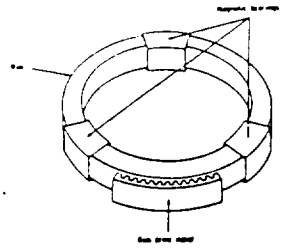

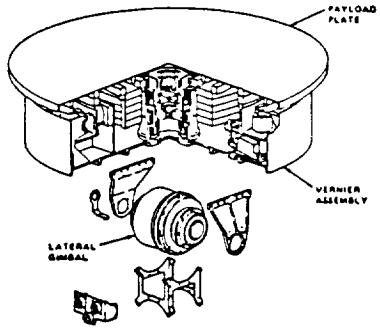


Annular Suspension and Pointing System

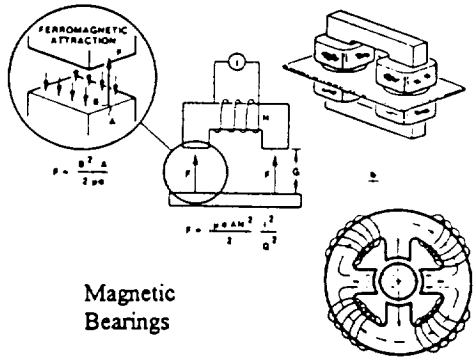


Magnetic Bearings

Large-Angle Magnetic Suspension Test Fixture (LAMSTF)

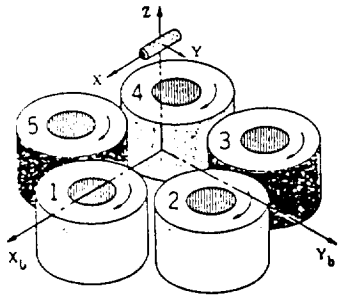


Maglev

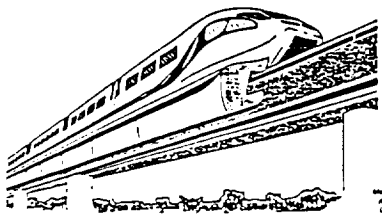

Maglifter

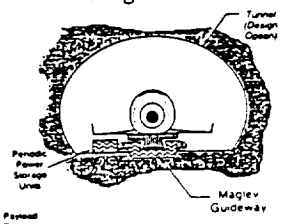


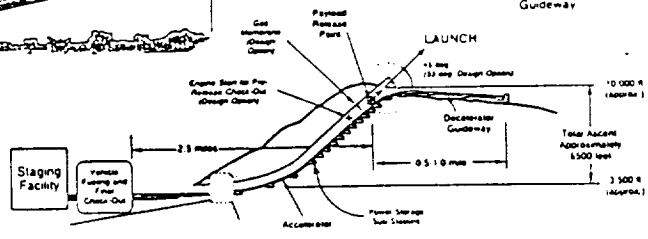

Appendix C

Britcher, C.P.: Application of magnetic suspension technology to large scale facilities.
Presented at AIAA 35th Aerospace Sciences meeting, Reno, NV, January 1997.
AIAA 97-0346

# Application of Magnetic Suspension Technology to Large Scale Facilities - progress, problems and promises

Colin P. Britcher*
Department of Aerospace Engineering
Old Dominion University
Norfolk, VA 23529-0247

## [1]Abstract

This paper will briefly review previous work in wind tunnel Magnetic Suspension and Balance Systems (MSBS) and will examine the handful of systems around the world currently known to be in operational condition or undergoing recommissioning. Technical developments emerging from research programs at NASA and elsewhere will be reviewed briefly, where there is potential impact on large-scale MSBSs. The likely aerodynamic applications for large MSBSs will be addressed, since these applications should properly drive system designs. A recently proposed application to ultra-high Reynolds number testing will then be addressed in some detail. Finally, some opinions on the technical feasibility and usefulness of a large MSBS will be given.

## Introduction

Wind tunnel Magnetic Suspension and Balance Systems (MSBS) have been under investigation and development by many organizations since 1957. A significant number of small-scale systems have been constructed and a variety of aerodynamic testing has been carried out[1]. Due to the undoubted technical challenges inherent in these systems, they have never been adopted for large-scale production testing. On the other hand, the idea is still too promising to abandon.

Current work in the U.S. is rather limited, but includes a serious investigation of a potential application for an "ultra-high Reynolds number" wind tunnel and a modest system recommissioning effort. The work is benefitting from a variety of "spin-off's" from generic large-gap magnetic suspension development work at NASA Langley Research Center, as well as technological progress in superconductivity and magnetic materials. Other work on MSBSs is currently known to be proceeding in Japan, Taiwan, P.R. China, England and Russia, with interest also being shown in other countries.

## Wind Tunnel Magnetic Suspension and Balance Systems

An aerodynamic test model can be magnetically suspended or levitated in the test section of a wind tunnel, as illustrated in Figure 1. The classical approach involves the use of a ferromagnetic core in the model, of either soft iron or permanent magnet material, with the applied fields generated by an array of electromagnets surrounding the test section. This arrangement is always open-loop unstable in at least one degree-of-freedom, so the position and attitude of the model is continuously sensed, with the electromagnet currents adjusted via a feedback control system to maintain stability and the desired position/orientation, as shown in Figure 2. Optical sensing systems of various types have been prevelant, although electromagnetic and X-ray systems have also been used. Electromagnet power amplifers typically require modest bandwidths, but high reactive power capacity. The resulting system is referred to as a Magnetic Suspension and Balance System (MSBS), since aside from the suspension/levitation function, whole-body forces and moments can be recovered from calibrations of the electromagnet currents.

The governing equations for this type of suspension system can be written as follows[2] :

$$\vec{F}_c \approx \forall \left( \vec{M} . \nabla \vec{B}_o \right) \qquad -(1)$$

$$\vec{T}_c \approx \forall \left( \vec{M} \times \vec{B}_o \right) \qquad -(2)$$

- where $\vec{M}$ represents the magnetization of the magnetic core in $A/m$, $\vec{B}$ the applied magnetic field in



*Associate Professor, Department of Aerospace Engineering, Senior Member, AIAA

Tesla, $\forall$ is the volume of the magnetic core in $m^3$, and the subscript $o$ indicates that the field or field gradient is evaluated at the centroid of the magnetic core. Now, following the detailed development presented elsewhere[2], the effect of changes in relative orientation between the magnetic core and the electromagnet array can be incorporated as follows :

$$\vec{F}_c \approx \forall [T_m][\partial B][T_m]^{-1}\vec{M} \qquad -(3)$$

$$\vec{T}_c \approx \forall \vec{M} \times \left[[T_m]\vec{B}\right] \qquad -(4)$$

Where a bar over a variable indicates magnetic core coordinates, [$\partial$B] is a matrix of field gradients and [$T_m$] is the coordinate transformation matrix from electromagnet coordinates to suspended element (magnetic core) coordinates. Study of equations 2 and 4 reveals that, with a single magnetization direction it is only possible to generate 2 torque components by this "compass needle" phenomena. This gives rise to the well-known "roll control" problem in wind tunnel MSBSs, where the magnetization direction has usually been along the long axis of the magnetic core, in turn along the axis of the fuselage. Roll torque can be generated by a variety of methods involving tranverse magnetizations, or by applications of second-order field gradients to model cores with reduced levels of symmetry.

In wind tunnel applications, the primary motivation for MSBSs has been the elimination of the aerodynamic interference arising from mechanical model support systems[3]. The fact that the suspended model forms part of a feedback control system inherently permits predetermined motions of the suspended model to be created rather easily. This suggests great potential for studies of unsteady aerodynamic phenomena, although this potential has not been fully exploited at this time.

It should be noted that the configuration discussed above is not the only possibility. Inherently stable configurations are feasible, such as by using a.c. applied fields, or by inclusion of diamagnetic materials in various ways. Laboratory suspensions using these techniques have been demonstrated for many years, but not in configurations relevant to the wind tunnel application. A major disadvantage has been the difficulty of arranging significant passive damping of unwanted motions. The feedback controlled approach relies on artificial damping, whose value is limited principally by the control algorithm and the power supply capacity.

## Current Research - United States

Ultra-High Reynolds Number Wind Tunnel MSBS

Research has been underway for several years examining the possibility of constructing an ultra-high Reynolds number "wind" tunnel with liquid helium as the working fluid. A Workshop was held in 1989 to coordinate early efforts[4]. At one point, the tunnel was referred to by some researchers as the "infinite Reynolds number" tunnel, since operation with superfluid helium was contemplated and a promise of effectively zero viscosity of the working fluid was held out. Current work appears to be focussed on slightly more modest performance (finite Reynolds number!) but could still result in a facility with a Reynolds number capability one order of magnitude higher than anything currently existing. Scientific application of a tunnel of this type could provide experimental data which is currently unobtainable, such as concerning high Reynolds number flows, particularly the evolution and decay of turbulence. The engineering application is clearly to hydrodynamic studies of submersibles, with a particular item of interest being wake-related signature reduction. It has been assumed that an MSBS would be mandatory for this type of facility, since a conventional support system would create severe problems by corruption of the test article's wake.

An alternative avenue of development appears to be an ultra-high pressure wind tunnel, with normal temperature air as the working fluid[5]. This approach poses a rather different set of design challenges, perhaps of a more traditional nature.

Research is proceeding, with recent completion of a candidate preliminary design and the hosting of a second Workshop[6,7].

The ODU 6-inch MSBS

If this system were to be described as the ODU/NASA/MIT 6-inch system, then its history and identity would be clear to all workers in the MSBS field. The electromagnet assembly and low-speed wind tunnel, shown in Figure 3, from the original MIT "6-inch" MSBS[8,9] has found its way to Old Dominion University via NASA Langley Research Center[10], and is currently in process of partial recommissioning. A unique feature is the use of Electromagnetic Position and attitude Sensing (EPS). It is planned to gradually restore the system to full operation with new power supplies and a digital control system.

The NASA Langley 13-inch MSBS

This system, illustrated in Figure 4, is still in operational condition, although has been inactive since 1992. During its use at LaRC it has been used for a variety of drag studies of axisymmetric and near-axisymmetric geometries, as well as support interference evaluations. Support interference increments on model drag of up to 200% were discovered, although this is hardly typical[11,12].

Large-Gap Magnetic Suspension Systems

A program has been underway for some years at NASA Langley Research Center to develop technology for large air-gap magnetic suspensions. Applications include, but are not limited to, wind tunnel MSBSs, space payload pointing and vibration isolation systems, momentum storage and control devices, maglev trains and electromagnetic launch systems. Two small laboratory scale levitation systems have been constructed, shown in Figures 5,6, with air-gaps between suspended element and electromagnets of 10 cm[13,14]. A larger system of comparable configuration, the Large-Gap Magnetic Suspension System (LGMSS), is close to completion, with a 1 meter air-gap[15]. This system includes superconducting coils to provide the background levitation force, with water-cooled copper control coils. It will represent the largest, large-gap magnetic suspension or levitation device ever constructed.

## Current Research - Rest of the World

Low-density, high Mach number aerodynamic measurements have been made for many years at Oxford University in England with their nominally 15 cm system. This system is arguably a "production" facility, since the main interest has been in the aerodynamic data generated, rather than the MSBS itself. Work is continuing up to the present time[16,17].

The National Aerospace Laboratory in Japan currently operates the largest MSBS ever constructed, with a test section 60 cm square (roughly 2 feet). Together with a smaller system (15 cm), current research is focussing on rapid force and moment calibration procedures[18].

Researchers in Taiwan have recently completed construction of a small (10 cm) system and are commencing low-speed wind tunnel tests[19]. Plans for larger systems are being discussed.

Russian activity is at a low level, but includes recent studies of data telemetry systems from suspended models. Current information suggests that one MSBS remains operational, at TsAGI[20].

A notable recent development has been the discovery of significant activity in P.R. China, about which information has just become available[21].

Some details concerning the abovementioned systems is given in Table I.

## Aerodynamic Test Requirements and Capabilities

A fresh look at the inherent capabilities of MSBSs and perceived shortcomings in conventional wind tunnel test capability was recently undertaken (unpublished). The main points will be summarized here, with the important rider that they should be taken to represent only an expression of the personal views of this author.

The large system design studies undertaken in the 1980's, under the direction of NASA Langley Research Center, concentrated on application to a large, high Reynolds number, transonic wind tunnel. The main technical justification was the elimination of support interference, which is a major problem around the transonic regime. Design studies were made for large-scale systems by General Electric Company[22] and later by Madison Magnetics Incorporated[23,24,25], illustrated in Figure 7. The conclusions were that a very large system was technically feasible, though quite expensive. A major cost driver was the unsteady (control) force and torque requirement, producing large cryogen boil-off in conventional superconducting electromagnets.

It seemed (and indeed is) inevitable that the cost of a "large MSBS" would be a significant fraction of the cost of the wind tunnel in which it would be used. The system under consideration would have provided static aerodynamic data, free of support interference, but little else. The technical risk was perceived to be quite high, since the system would have been around 5 times larger in linear dimension than anything previously attempted (c.1985, NAL 23-inch system and NASA LaRC LGMSS not yet completed). The design was ultimately seen as constituting an insufficiently attractive program and work gradually slowed and eventually was stopped, in or around 1990.

Provision of an support interference-free aerodynamic test capability is a valuable goal and should be pursued. However, the precise application needs to be carefully considered. For instance, while there is no doubt that

support interference is major problem in the accurate evaluation of cruise drag in wind tunnel testing, there often exist strategies for its assessment, such as mounting normally sting-mounted models on blade, wing-tip or fin supports[26]. This is an expensive process, but it is difficult to construct a persuasive argument this should be replaced by another apparently expensive process (MSBS). Valuable generic data could, however, be generated at moderate Reynolds numbers in a smaller and less expensive facility. Some interesting information was generated using the 13-inch MSBS at LaRC, which included a demonstration of the fact that the drag correction for sting interference could be as high as 200% (though admittedly not typical, as mentioned previously[11,12]). It has also been known for some time that support interference can be particularly significant in cases where the support lies in a separated and/or unsteady wake or any type of vortex flows[27,28]. The understanding of high angle-of-attack and unsteady aerodynamics would be greatly improved by the provision of interference-free test data, especially with the possibility of including fully representative model motions, such as wing rock. The fundamental research to permit the use of MSBSs at high angles-of-attack has been done, and suspension at extreme attitudes has been demonstrated, but the systems have not yet been systematically applied to this type of testing.

## New Technology

New Configurations

An important novel feature of the LGMSS configuration is the use of a transversely magnetized permanent magnet core in the cylindrical suspended element. This can provide full six degree-of-freedom control capability. The additional torque is generated by a term of the form :

$$\vec{T}_z \approx V \int_V \vec{M}_z \left\{ \frac{\partial B_y}{\partial z} x \right\} \qquad -(5)$$

This can be non-zero if the core geometry is suitably chosen and $\frac{\partial}{\partial x}\left\{\frac{\partial B_y}{\partial z}\right\}$ is non-zero. It should be noted that this configuration is well suited to the wind tunnel application, where generation of magnetic roll torque has been a long-standing problem. Using vertically magnetized permanent magnet cores within the fuselage provides roughly equal (and large) pitch and roll torque capability. Lift, drag and sideforce capability will be largely unaffected compared to the conventional axial magnetization configuration. Only yaw torque is relatively reduced, although it is observed that aerodynamic yaw torques are seldom dominant. The proposed new arrangement is shown in Figure 8.

Electromagnets and Magnetic Materials

The forces and moments generated by a conventional MSBS tend to be proportional to the strength of the magnetic fields generated by the electromagnets external to the tunnel flow and the magnetic moment of the suspended element. The suspended element can have a magnetic core of soft iron or permanent magnet material. The former promises higher absolute levels of magnetization, but requires an external "magnetizing" field, and also presents some difficuties with system calibration, since the magnetization is not absolutely fixed. Within the last few months, information concerning a new permanent magnet material, doped acicular iron powder, has been widely circulated[29]. The claimed specifications of this new material suggest a doubling of some aspects of performance from anything previously available. Specifically, magnetization intensities well above 2 Tesla are claimed, whereas current Nd-Fe-Bo materials achieve about 1.2 Tesla. Should this prove to be realised in practice, the technical and economic feasibility of MSBSs will be profoundly improved.

Turning now to the external electromagnets, progress in the development of practical high temperature superconductors continues to be steady and impressive. Small a.c. electromagnets have been fabricated and are being tested in magnetic bearing and other applications. Although future progress is not predictable, it seems likely that high temperature superconducting electromagnets will soon be feasible options at least for small and medium-scale wind tunnel MSBSs.

It can also be noted that magnetic suspension and levitation technology has made dramatic progress in other applications in recent years. Feedback-controlled magnetic bearings for rotating machinery are a viable commercial item[30], with a growing number of companies involved and regular International Symposia. Useful spin-offs from this work include specialized control hardware, algorithms and software, new sensing approaches, improved system modelling and analysis, and application of High Temperature Superconductors (HTS) to current-controlled electromagnets. Maglev "trains" are on the verge of revenue-generating operation, with sophisticated prototypes in operation in Germany and Japan. The German approach relies on feedback controlled copper

electromagnets generating attractive levitation forces from below the "guideway" (track); the Japanese approach utilizes superconducting electromagnets generating repulsive levitation forces by inducing eddy currents in the guideway. Both approaches have a speed capability in excess of 300 m.p.h. The U.S. National Maglev Initiative (now defunct) spawned a range of design studies, with the Grumman Corporation hybrid magnet design perhaps notable.

## Preliminary Considerations for MSBS Application to Ultra-High Reynolds Number Facilities

The magnitude of the engineering challenge of an MSBS is determined primarily by the aerodynamic test requirements and the choice of working fluid. By way of example, three low temperature design points and one high pressure design point have been chosen for a 10:1 length-to-diameter ratio quasi-axisymmetric, low-drag model. The target length Reynolds number is $10^9$. Numerical values are derived largely from data in reference 4. The model weight is estimated based on the weight of a steel or permanent magnet magnetic core occupying around 50% of the available volume. The drag force is estimated based on a drag coefficient ($C_D$) of 0.1. Results are shown in Table II.

The immediate conclusion is that this application is extremely benign from the perspective of aerodynamic forces and moments. The likely aerodynamic or hydrodynamic forces appear to be a small fraction of the deadweight of the model. This fact justifies some attention to passively stable suspensions in this application[6]. Increasing attention is being paid to this possibility by the magnetic bearing community and progress is being made, although many difficulties remain to be solved[31].

Turning to more detailed engineering design issues, the first consideration for this application is the extremely low temperature. Whatever the working fluid, an MSBS for helium tunnels must either be designed for an environment around 2-4 K, or the test section must be designed such that the MSBS is essentially "outside" the cold zone. The latter approach was taken with the only MSBS to be used with a cryogenic wind tunnel to date[32]. It is thought, however, that the former would be preferable in this application, due to the extreme penalty in cooling power incurred should the thermal insulation of the test section be compromised. Immediately one might be concerned that the power dissipation of the suspension electromagnets might negate this advantage, but a.c. capable low-temperature and high-temperature superconducting coils have been demonstrated. HTS coils are perhaps the first choice, since they would be operated well below their transition temperature, providing huge stability margins and permitting considerable flexibility in design of cooling and insulation systems. The d.c. and a.c. field requirements in this application appear to be extremely modest compared to "conventional" wind tunnel MSBSs, suggesting no great problems in electromagnet or power supply design or procurement. In the case of an MSBS for a high pressure air tunnel, a similar design challenge is faced. Here, the MSBS must be placed inside the pressure shell, or the pressure shell must be designed such that it can easily be penetrated by magnetic fields. Due to the very high pressures involved, the latter option is probably the first choice (keeping the diameter of the pressure shell to a minimum), and seems feasible if composite materials are used. Conducting materials cannot be used extensively between the electromagnets and the suspended model, due to the induction of eddy currents by time-varying magnetic fields.

Two approaches for position and attitude sensing are viable, optically-based and the electromagnetic position sensor[8,9]. Optoelectronic devices can operate effectively at 2-4 K, or at high pressures, but there are practical concerns relating to condensation of stray gases and penetration of the pressure shell. For this reason, and also due to the perception that the typical model to be tested is naturally quasi-axisymmetric, and does not seem likely to be oriented at extreme angles relative to the test section axis, the EPS is recommended as a first choice. Here, the EPS coils could, perhaps should, be located inside the main structure of the wind tunnel. The electromagnetic behaviour of this system should be essentially independent of pressure or temperature changes.

The ferromagnetic core of the model could be either soft iron or permanent magnet. It is known that either will operate without difficulty down to liquid nitrogen temperature, in fact exhibiting improved properties. Operation at the extremely low temperatures anticipated would have to be researched. There seems little point in resorting to the persistant superconducting solenoid model core[25,32] since the force requirements seem so modest. The main purpose of this core design was to provide higher force capability in high dynamic pressure wind tunnel applications.

## Some Opinions and Observations

It seems that a argument can be made that the earlier focus on large, high Reynolds number, transonic wind tunnels was flawed, insofar as the "cost-benefit ratio" for a system focused largely on support interference elimination in static testing was never favorable. Instead, it is now argued, at least by this author, that the focus should be on the areas of unsteady aerodynamics and dynamic stability, where conventional test facilities are arguably quite deficient. The unique ability of MSBSs to permit controlled motion through arbitrary trajectories (limited only by force and moment capability) represents an enormous untapped potential.

At least three research teams have addressed dynamic stability testing over the years, though none recently. At MIT[9,33] and the University of Southampton[34,35], forced oscillation testing has been successfully carried out. The University of Virginia developed a special design of MSBS specifically for dynamic stability work[36,37] and conducted limited testing. With more modern control and data acquisition approaches, small-amplitude forced oscillation testing in an MSBS should be a quite viable test technique. A single facility could make measurements requiring an array of conventional mechanical rigs. Although not so far pursued beyond the point of speculation, "modal" testing (i.e. directly forcing model motion in representative natural modes) or on-line system identification with random excitation might prove to be viable alternative approaches.

## Acknowledgements

This work was partially supported by NASA Langley Research Center, Guidance and Control Branch, Flight Dynamics and Control Division, under Grant NAG-1-1056. The Technical Monitor was Nelson J. Groom.

## References

1. Tuttle, M.H.; Moore, D.L.; Kilgore, R.A.: Magnetic suspension and balance systems - a comprehensive annotated bibliography. NASA TM-4318, August 1991; supercedes TM-84661, July 1983

2. Groom, N.J.; Britcher, C.P.: Open-loop characteristics of magnetic suspension systems using electromagnets mounted in a planar array. NASA TP-3229, November 1992.

3. Tuttle, M.H.; Lawing, P.L.: Support interference of wind tunnel models - a selected annotated bilbiography. Supplement to NASA TM-81909, May 1984

4. Donnelly, R. (ed.): High Reynolds number flows using liquid and gaseous helium. Proceedings of the 7th Oregon Conference on Low-Temperatue Physics, published by Springer-Verlag, 1991.

5. Zagarola, M.; Smits, A.; Yakhot, V.; Orszag, S.: Experiments in high Reynolds number turbulent pipe flow. AIAA 34th Aerospace Sciences Meeting, January 1996, AIAA 96-0654

6. Smith, M.R.; Eyssa, Y.M.; Van Sciver, S.W.: Design of a superconducting magnetic suspension system for a liquid helium flow experiment. 3rd International Symposium on Magnetic Suspension Technology, Tallahassee, FL, December 1995. NASA CP-3336, July 1996.

7. Donnelly, R. (ed.): Proceedings of the international workshop on ultra-high Reynolds number flows, Brookhaven National Laboratory, June 1996. To be published by American Institute of Physics / Springer-Verlag.

8. Stephens, T.: Design, construction and evaluation of a magnetic suspension and balance systems for wind tunnels. NASA CR-66903, November 1969.

9. Covert, E.E.; Finston, M.; Vlajinac, M.; Stephens, T.: Magnetic balance and suspension systems for use with wind tunnels. Progress in Aerospace Sciences, vol.14, 1973.

10. Schott, T.; Jordan, T.; Daniels, T.: Status of the MIT/NASA 6 inch MSBS. International Symposium on Magnetic Suspension Technology, Hampton, August 1991. Published as NASA CP-3152, 1992.

11. Britcher, C.P.; Alcorn, C.W.: Subsonic sting interference on the aerodynamic characteristics of a family of slanted-base ogive-cylinders. NASA CR-4299, June 1990.

12. Britcher, C.P.; Alcorn, C.W.: Interference-free measurements of the subsonic aerodynamic of slanted-base ogive-cylinders. AIAA Journal, April 1991.

13. Britcher, C.P.; Ghofrani, M.: A magnetic suspension system with a large angular range. Review of Scientific Instruments, July 1983.

14. Cox, D.; Groom, N.J.: Implementation of a decoupled controller for a magnetic suspension system using electromagnets mounted in a planar array. 2nd International Symposium on Magnetic Suspension Technology, Seattle, WA, August 1993. NASA CR-3247, May 1994.

15. Groom, N.J.: Description of the large gap magnetic suspension system ground based experiment. Technology 2000. NASA CP-3109, 1991.

16. Smith, R.W.; Lord, R.G.: Drag and lift measurements on inclined cones using a magnetic suspension and balance. 16th International Conference on Rarefied Gas Dynamics, July 1988.

17. Dahlen, G.A.; Brundin, C.L.: Wall temprature effects on rarefied hypersonic cone drag. Rarefied Gas Dynamics, Vol.1, Plenum, 1985.

18. Sawada, H.; Suenaga, H.; Kunimasu, T; Kohno, T.: Status of MSBS research at NAL in 1995. 3rd International Symposium on Magnetic Suspension Technology, Tallahassee, FL, December 1995. NASA CP-3336, July 1996.

19. Lin, C.E.; Sheu, Y.R.; Jou, H.L.: Magnetic levitation system design and implementation for wind tunnel application. 3rd International Symposium on Magnetic Suspension Technology, Tallahassee, FL, December 1995. NASA CP-3336, July 1996.

20. Kuzin, A.; Shapovalov, G.; Prohorov, N.: Force measurements in magnetic suspension and balance system. 3rd International Symposium on Magnetic Suspension Technology, Tallahassee, FL, December 1995. NASA CP-3336, July 1996.

21. Ji, S.; Yin, L-M.; Xie, Z.: An investigation into the set-ups for the magnetic suspension and balance system for wind tunnels. 1st International Congress on Experimental Fluids Mechanics, Chengdu, China, June 1991.

22. Bloom, H.; et al.: Design concepts and cost studies for magnetic suspension and balance systems. NASA CR-165917, July 1982.

23. Boom, R.W.; Eyssa, Y.M.; McIntosh, G.E.; Abdelsalam, M.K.: Magnetic suspension and balance system study. NASA CR-3802, July 1984.

24. Boom, R.W.; Eyssa, Y.M.; McIntosh, G.E.; Abdelsalam, M.K.: Magnetic suspension and balance system advanced study. NASA CR-3937, October 1985.

25. Boom, R.W.; Abdelsalam, M.K.; Eyssa, Y.M.; McIntosh, G.E.: Magnetic suspension and balance system advanced study - Phase II. NASA CR-4327, November 1990.

26. Carter, E.C.: Interference effects of model support systems. In AGARD-R-601, April 1973.

27. Dietz, W.E., Jnr.; Altstatt, M.C.: Experimental investigation of support interference on an ogive cylinder at high incidence. 16th AIAA Aerospace Sciences meeting, January 1978.

28. Uselton, B.L.: Sting effects as determined by the measurement of pitch-damping derivatives and base pressures at Mach 3. 10th AIAA Aerodynamic testing conference, San Diego, April 1978.

29. Sciex, U.K. Ltd.; also www.magnetweb.com

30. Schweitzer, G.; Bleuler, H.; Traxler, A.: Active magnetic bearings. Hochschulverlag AG, 1994.

31. Moon, F.: Superconducting levitation. Wiley 1994.

32. Britcher, C.P.: Progress towards magnetic suspension and balance systems for large wind tunnels. AIAA Journal of Aircraft, April 1985.

33. Vlajinac, M.: Aerodynamic characteristics of axisymmetric and winged model configurations using a magnetic suspension and balance system. 2nd International Symposium on Electro-Magnetic Suspension, July 1971.

34. Abdel-Kawi, S,; Diab, T. A.G.; Goodyer, M.J.; Henderson, R.L.; Judd, M.: Aerodynamic data acquisition with the University of Southampton magnetic balance. 2nd International Symposium on Electro-Magnetic Suspension, July 1971.

35. Goodyer, M.J.: The six component magnetic suspension system for wind tunnel testing. High reynolds number flows and liquid helium. Springer-Verlag, 1992.

36. Ragunath, B.S.; Parker, H.M.: Evaluation of aerodynamic derivatives from a magnetic balance system. NASA CR-112305, 1972.

37. Bharathan, D.; Fisher, S.S.: Stability derivative measurements with magnetically suspended cone-cylinder models. 15th AIAA Aerospace Sciences meeting, December 1977.

Table I - "Operational" MSBSs, 1996/7

| Organization | Approx. Test Section Size | Current Application | Current Status |
|---|---|---|---|
| NASA Langley Research Center | 13-inch | Low-speed, R&D | Inactive |
| Old Dominion University | 6-inch | System R&D | Recommissioning |
| Oxford University | 3-inch | Hypersonic aerodynamics | Active |
| MAI/TsAGI, Moscow | 18-inch | System R&D | Inactive |
| NAL, Japan | 4-inch | System R&D | Active |
| NAL, Japan | 23-inch | System R&D | Active |
| NCKU, Taiwan | 6-inch | System R&D | Active |
| CIT/CARDC, P.R. China | 6-inch | System R&D | Active |

Table II - Characteristics of Candidate Designs for Ultra-High Reynolds Number Wind Tunnels

| | Gaseous Helium | Helium I | Helium II | High Pressure |
|---|---|---|---|---|
| Temperature, K / Pressure, atmospheres | 5.3 / 1 | 2.8 / 1 | 1.6 / 1 | 300 / 100 |
| Velocity, m/s | 40 | 10 | 4 | 48.4 |
| Unit Reynolds No., $m^{-1}$ | $3 \times 10^8$ | $3.8 \times 10^8$ | $4.4 \times 10^8$ | $3.3 \times 10^8$ |
| Dynamic pressure, Pa | 8725 | 7150 | 1160 | 288,000 |
| Model length, m | 3.3 | 2.63 | 2.27 | 3.0 |
| Test section size, m | 0.94 square | 0.75 square | 0.65 square | 0.85 square |
| Max. model weight, N | 8700 | 4400 | 2830 | 7190 |
| Drag force, N | 74.6 | 38.9 | 4.7 | 2992 |

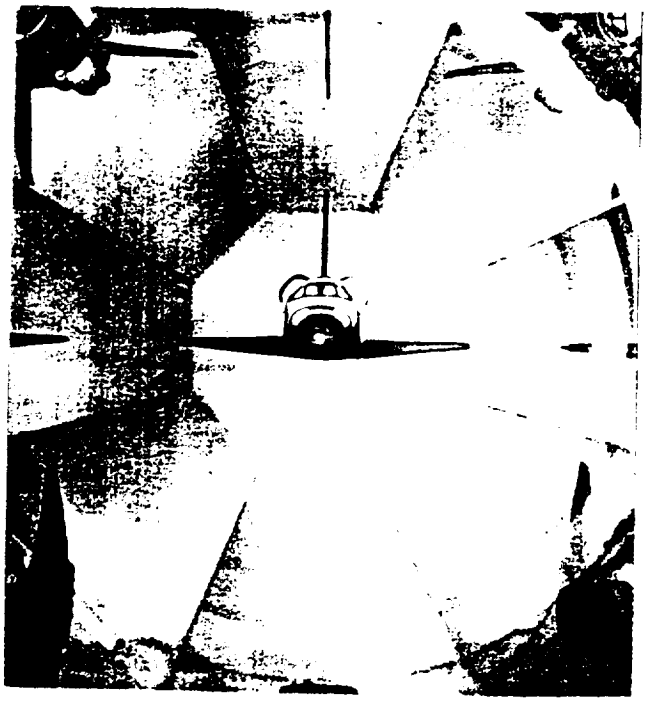

Figure 1 - Wind Tunnel Magnetic Suspension and Balance System (ODU 6-inch MSBS)

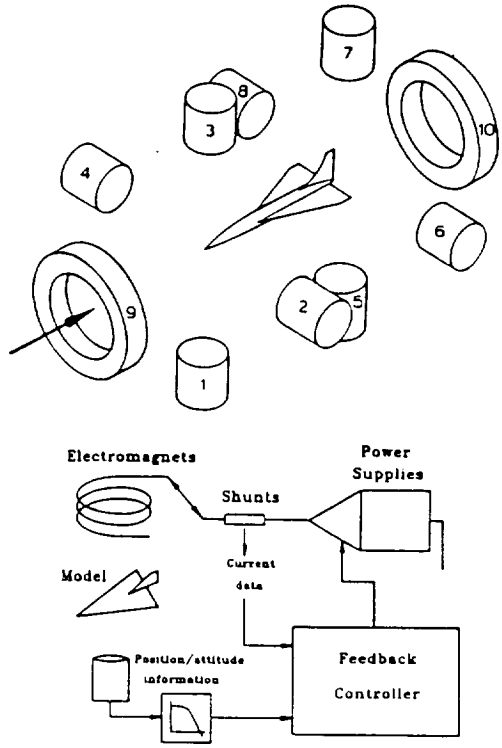


Figure 2 - Generic Configuration and System Block Diagram for a Wind Tunnel MSBS

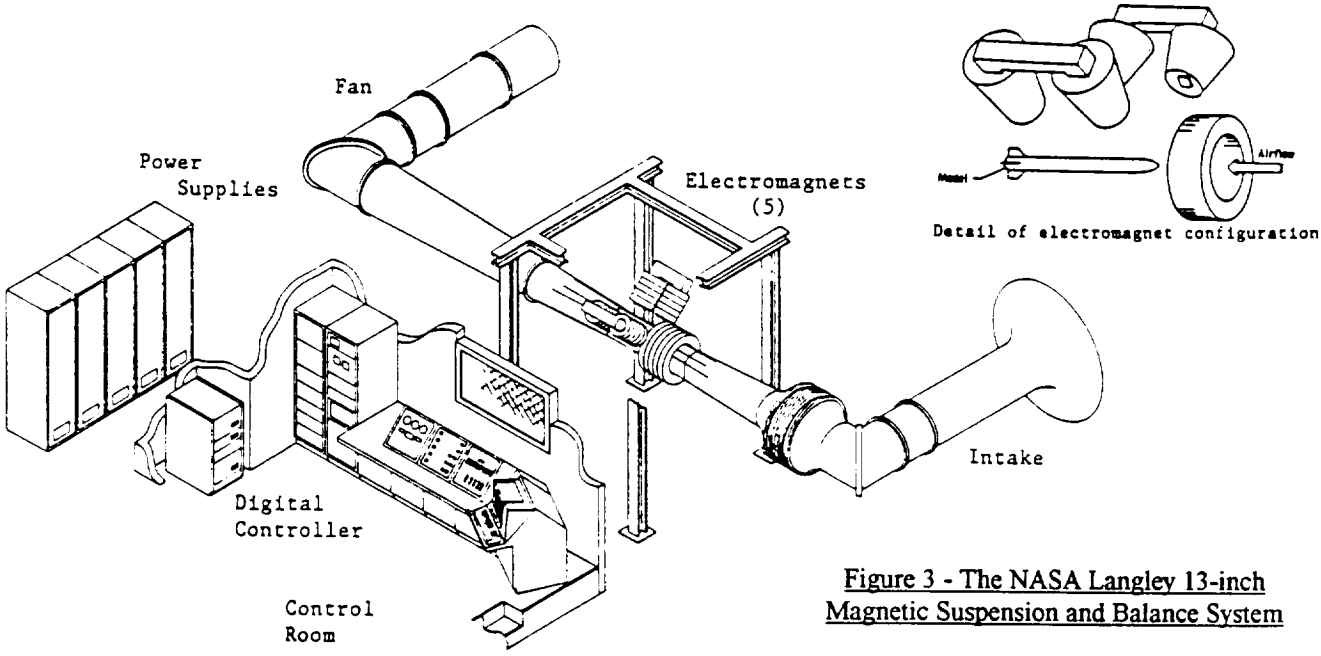


Figure 3 - The NASA Langley 13-inch Magnetic Suspension and Balance System

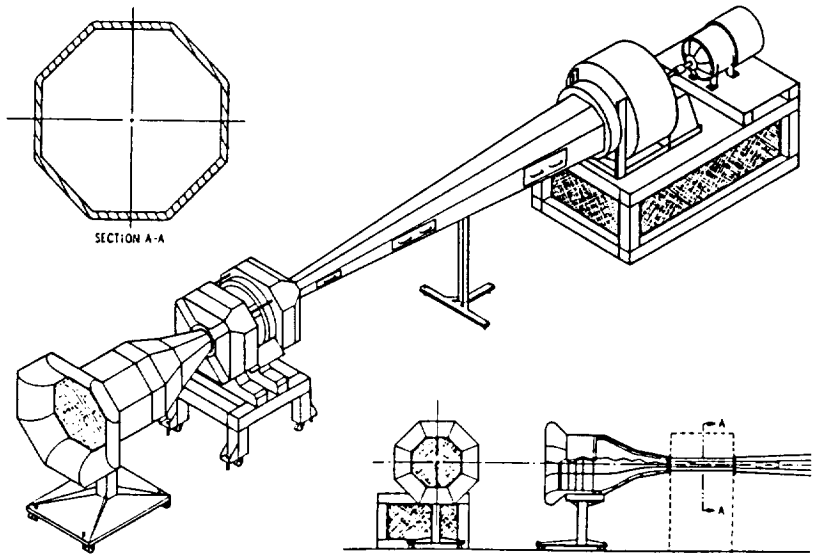


Figure 4 - The ODU/NASA/MIT 6-inch Magnetic Suspension and Balance System

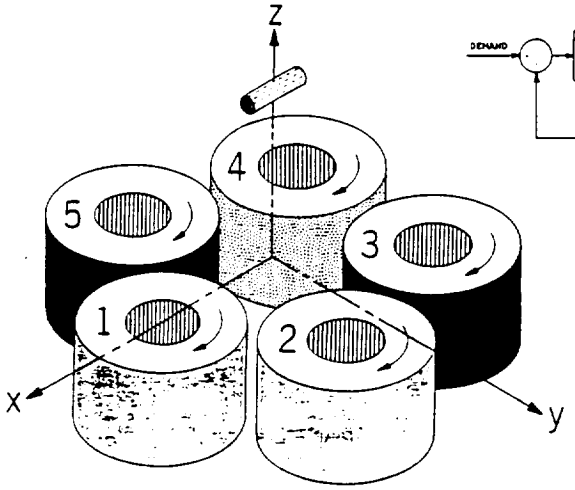


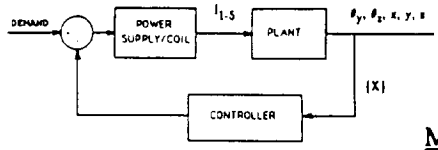


Figure 5 - The NASA LaRC Large Angle Magnetic Suspension Test Fixture (LAMSTF)

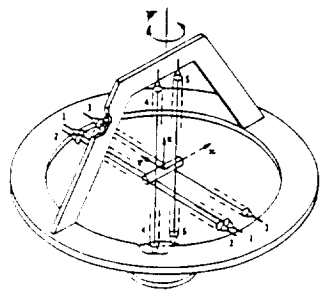

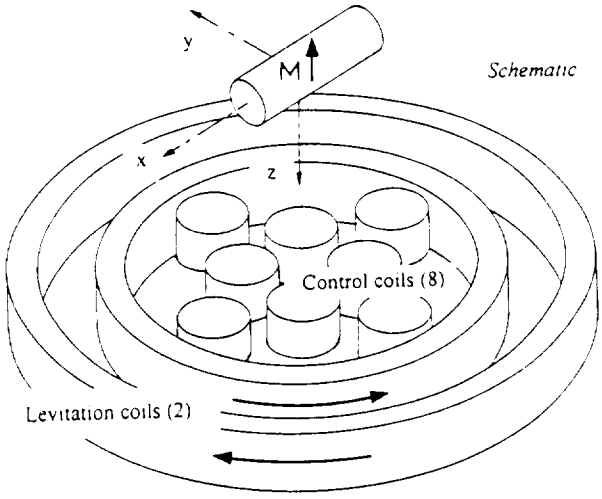


Figure 6 - The 6 Degree-of-Freedom LAMSTF Electromagnet Configuration

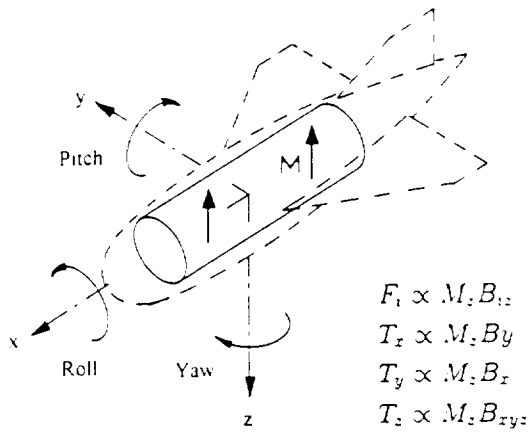


Figure 8 - Transverse Magnetization Configuration

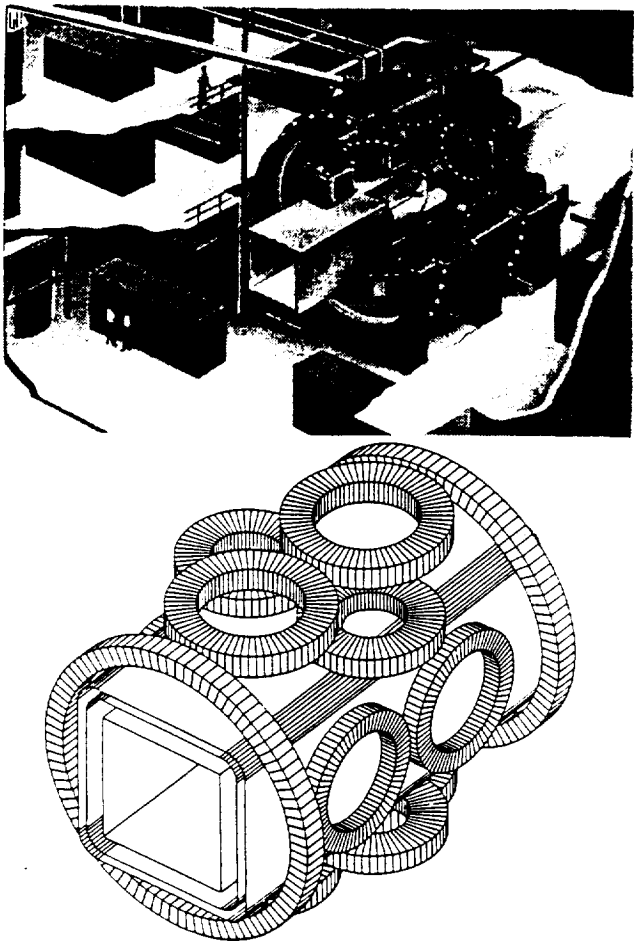

Figure 7 - Large System Design Studies, General Electric and Madison Magnetics

Appendix D

Britcher, C.P.: A new look at the Backers bearing.

# A New Look at the Backers Bearing

Colin P. Britcher
Department of Aerospace Engineering
Old Dominion University

## Abstract

The "Backers" bearing, first published in 1961, is a clever arrangement of permanent magnets intended to form a radial bearing. Layers of permanent magnets with alternating polarity and acting in repulsion (as originally proposed) are stacked, such that the number of unstable degrees-of-freedom of the assembly is reduced to one. The arrangement is unstable in axial translation only, requiring only one active control system or other form of restraint.

This paper presents some new thoeretical and computational analysis of this configuration, intended to provide more detailed design guidelines than those previously available. Some approximations made in the original papers are shown to be significantly in error.

## Introduction

The well-known theorem due to Earnshaw [1] shows that any magnetic suspension configuation comprised of ferromagnetic material must be unstable in at least one degree-of-freedom. This precludes the possibility of a fully stable passive bearing, relying on permanent magnets as the source of the magnetic field. Nevertheless, a variety of permanent magnet bearing configurations have been developed over the years, with various design features employed to reduce the number of unstable degrees of freedom. Notable among these, perhaps, are the permanent magnet-assisted bearings of the Charles Stark Draper Laboratory [2]. Here, the one or more unstable degrees-of-freedom were stabilized by a variety of means, mostly relying on self-tuning "internal" feedback mechanisms.

In 1960, F.T. Backers of the Philips Laboratory, proposed a journal bearing configuration which would be fully stable in the radial direction, as well as in rotations about transverse axes, and would be unstable only in the axial degree-of-freedom. This combination is a good match to some rotating machine applications, particularly where axial thrusts in the machine are large compared to other forces, which is often the case. An active axial bearing, or even a mechanical axial bearing, is required to complete the machine.

The Backers design [3] relies on a clever arrangement of stacked permanent magnet rings, magnetized radially, but with alternating polarity and acting in repulsion. The arrangement is illustrated in Figure 1. It should be noted that long cylindrical "sleeves", magnetized radially and acting in repulsion are relatively ineffective in generating radial forces, as well

as lacking stiffness about transverse axes. This is due to the fact that the magnetic flux midway between the inner and outer sleeves tends to zero as the sleeve length increases. The alternating polarity of the ring stack is thus an essential feature of the design.

Subsequent analyses have shown that equivalent forces can be generated by configurations with the direction of magnetization aligned axially, but still magnetized in alternating directions [4-7]. It is pointed out that this configuration is easier to manufacture.

## Analysis

Backers' original analysis models the radial bearing as an infinite sheet of magnetized material with a sinusoidal variation of magnetization, as illustrated in Figure 2. This is equivalent to "unrolling" a journal bearing with a clearance that is small with respect to the journal diameter. The assumption of sinusoidal variation of magnetization appears to have been made largely for convenience, although it may properly represent the practical case for the relatively low coercive force permanent magnet materials typically available at the time[1]. Modern high remenance, high coercive force materials, such as rare-earth cobalts and neodymium-iron-boron can be fabricated into assemblies such as those described herein with no appreciable loss or changes in magnetization.

Following Backers' analysis, some rather difficult derivation leads to :

$$\sigma_y = -\frac{J_o^2}{4\mu_o}\left(1-e^{-\frac{2\pi d}{\lambda}}\right)^2\left(e^{-\frac{2\pi g}{\lambda}}\right)Cos\left(\frac{2\pi z_o}{\lambda}\right) \qquad \text{- (1)}$$

- where $\sigma_y$ is the Maxwell normal stress in the airgap. The first term in brackets is close to unity for thick sheets of magnetic material. The cosine term will be a maximum at a half wavelength "offset" between the two magnetized sheets (to generate repulsive force between the sheets). This leads to :

$$\sigma_y|_{max} \approx \frac{J_o^2}{4\mu_o}\, e^{-\frac{2\pi g}{\lambda}} \qquad \text{- (2)}$$

Applying this result to a journal bearing, shown in Figure 3, straightforward application of geometry leads to :

$$g \approx c + eCos(\theta) \qquad \text{- (3)}$$

$$dF_r = \sigma_y\, LR\, d\theta \qquad \text{- (4)}$$

$$dF = -Cos(\theta)\, dF_r \qquad \text{- (5)}$$

$$F \approx -2\,LR \int_0^{\pi} Cos\theta \frac{J_o^2}{4\mu_o} e^{-\frac{2\pi(c+eCos\theta)}{\lambda}}\, d\theta \qquad \text{- (6)}$$

---

[1]Backers used low remenance, high coercive force Ferroxdure for the original validation experiments

Equation 6 is observed to give maximum force if $c = e$ (i.e. bearing is "bottomed out"). Making a substitution of :

$$b = \frac{2\pi c}{\lambda} \qquad \text{- (7)}$$

$$F \approx -\frac{J_o^2}{2\mu_o} LR \left( e^{-b} \int_0^{\pi} Cos\theta e^{-bCos\theta} d\theta \right) \qquad \text{- (8)}$$

Backers states that the term in brackets is a maximum "around" $b = 1$. This appears to be incorrect. Numerical analysis suggests a maximum closer to $b = 1.5$, and the true maximum may, in fact, occur at $b = \pi/2$. This would result in an optimally dimensioned bearing with $\lambda \approx 4 \times$ Radial clearance (Backers suggests 6). In physical terms, the "wavelength" of the magnatization distribution should be about 4 times the size of the airgap.

Further analysis by Backers suggests that higher forces will be obtained with a "square-wave" magnetization distribution. A revised estimate of the optimal value of $b$ is not given, however. Later analyses have suggested that a finite spacing between layers of magnetic material may result in improved performance. This is physically reasonable, since adjacent regions of magnetic materials with opposing directions of magnetization more-or-less cancel each other's external field. By adding airgaps between alternately magnetized layers, the least effective regions (adjacent opposite magnetizations) are eliminated.

## Numerical Analysis

Rather than pursue further theoretical analysis, it was decided to attempt a computational analysis of a 2-dimensional representation of the Backers bearing (a similar approach to the model discussed above). The objective would be to rapidly generate design information (orders-of-magnitude, trends and so forth), usable in practical problems.

A square-wave magnetization distribution was chosen, partly for convenience, also since this more closely represents the practical case of stacked high-performance magnets. A series of finite element models were created using the OPERA-3D finite element preprocessor, with subsequent analysis carried out using the TOSCA magnetostatic code. The 3D code can generate 2D solutions by proper choice of boundary conditions as illustrated in Figure 4. The baseline geometry actually corresponds to 20 mm by 20 mm[2] blocks, spaced variable distances apart and with a variable gap between the layers, as illustrated in Figure 5, but the optimum proportions of the magnet assembly are independent of scale.

---

[2]Arbitrarily chosen

The term "gap" is used to specify the air-gap between magnet layers, equivalent to the cleareance in a bearing. "Spacing" refers to the dead-space between adjacent magnet blocks in the same sheet (same side of the bearing gap). The lateral shift between the two magnet layers is described as "offset". Gap and offset can be non-dimensionalized based on the size of the magnet blocks, as shown in Figure 5. A large number of cases were run, covering a wide range of design variables.

## Results

Due to space limitations, only representative results will be presented here. Figure 6 shows the variation of repulsive force with spacing between magnet blocks. The optimal spacing[3] appears to be around 0.5, with the value increasing with increasing gap. Figure 7 shows the variation of repulsive force with gap for zero offset, indicating the approximately inverse gap-force relationship as expected, also the gradual reduction in repulsive force with increasing lateral offset between magnet layers. Results for non-zero offsets show similar trends, but with force levels decreasing with increasing offset. Figure 8 directly shows the reduction in repulsive force with increasing lateral offset, for a particular gap. The rate of decline per mm is more rapid for smaller spacing, since the wavelength of the assembly is lower. The rates of decline as a function of dimensionless offset are more nearly equal. Figure 9 shows the variation of lateral force with offset. The rate of increase of force per mm is similar in all cases, but again the wavelengths of the assemblies vary.

## Discussion and Interpretation of Results

In a practical application, a design constraint based on volume is usually important. This is often the total volume of the assembly, since available volume for a bearing installation is often restricted. However, the constraint could alternatively be based on the volume of the magnetic material. This latter case would broadly correspond to a minimum-weight or minimum-cost design, where the minimum quantity of magnetic material is used to satisfy a given force requirement, with low-cost, low-density filler material between the magnet blocks. The "optimum" configuration is different in each case.

---

[3]See later section for a discussion of what constitutes optimality

## References


1. Earnshaw, S.: On the nature of the forces that regulate the constitution of the luminiferous ether. Transactions of the Cambridge Philosophical Society, Vol. 7, 1839.
2. Frazier, R.H.; Gilinson, P.J.; Oberbeck, G.A.: Magnetic and Electric Suspensions. MIT Press, 1974.
3. Backers, F.T.: A Magnetic Journal Bearing. Philips Technical Review, Vol. 22, 1961
4. Yonnet, J-P.: Passive magnetic bearings with permanent magnets. IEEE Transactions on Magnetics, Vol-MAG-14, September, 1978.
5. Yonnet, J-P.: Permanent magnet bearings and couplings. IEEE Transactions on Magnetics, Vol-MAG-17, January 1981.
6. Yonnet, J-P.; Lemarquand, G.; Hemmerlin, S.; Olivier-Rulliere, E.: Stacked structures of passive magnetic bearings. Journal of Applied Physics, November 1991.
7. Marinescu, M.; Marinescu, N.: A new improved method for computation of radial stiffness of permanent magnet bearings. IEEE Transactions on Magnetics, September 1994.

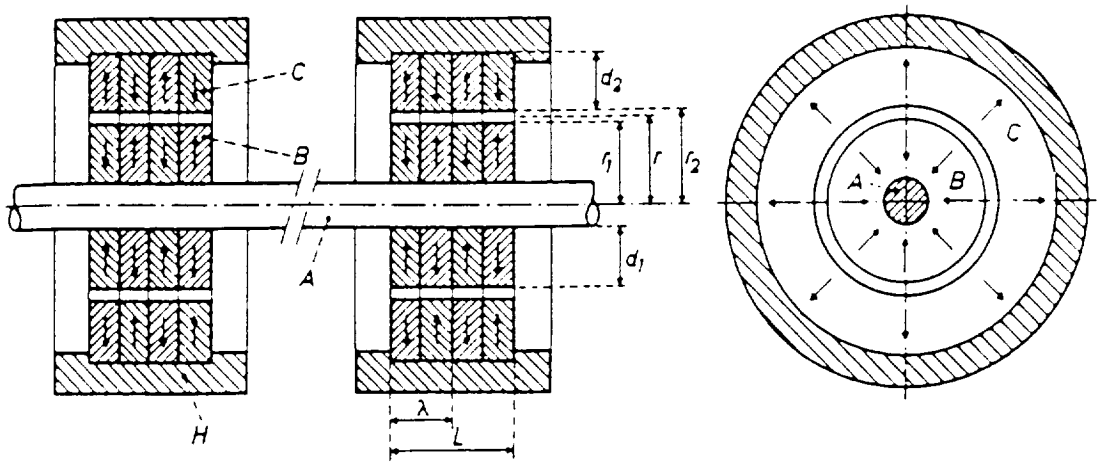


Figure 1 - The Backers Bearing Configuration

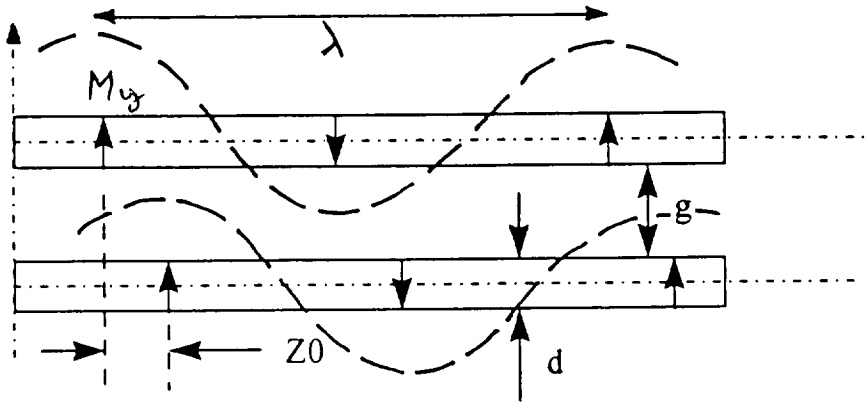


Figure 2 - Sinsusoidal Magnetization Distribution

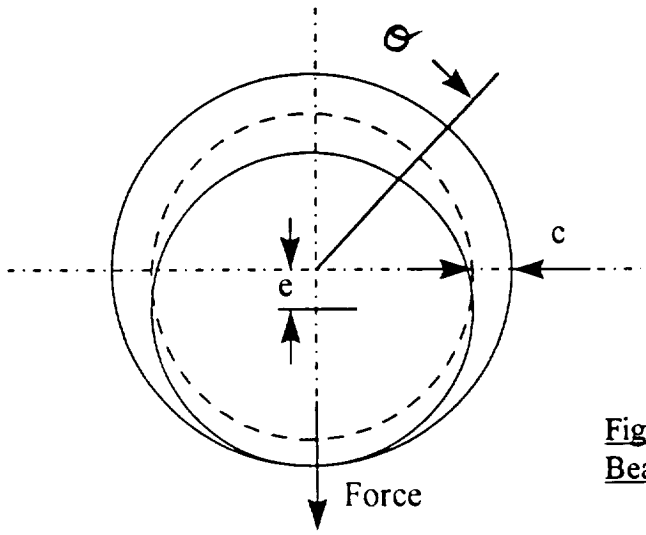


Figure 3 - A Journal Bearing Configuration

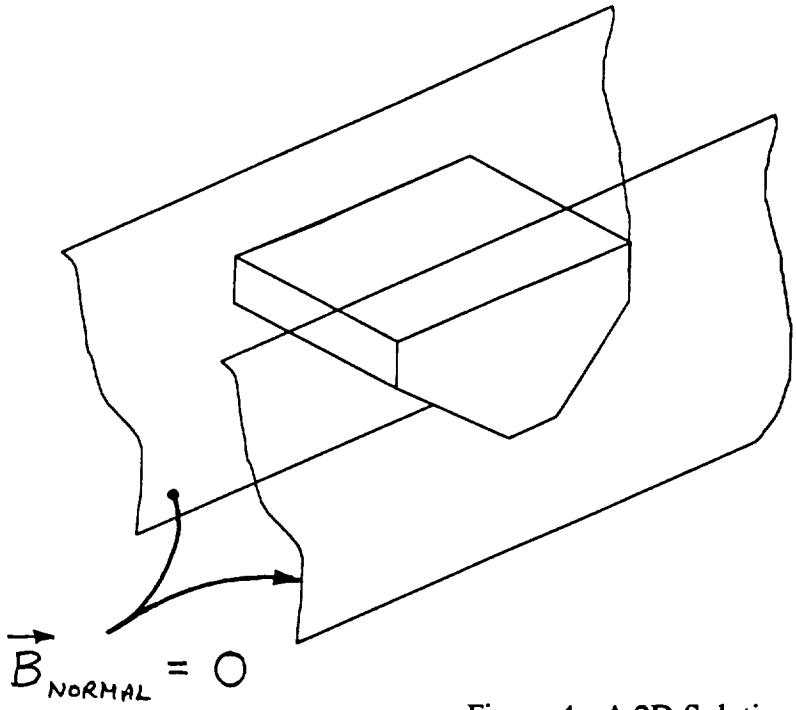


Figure 4 - A 2D Solution in a 3D Environment

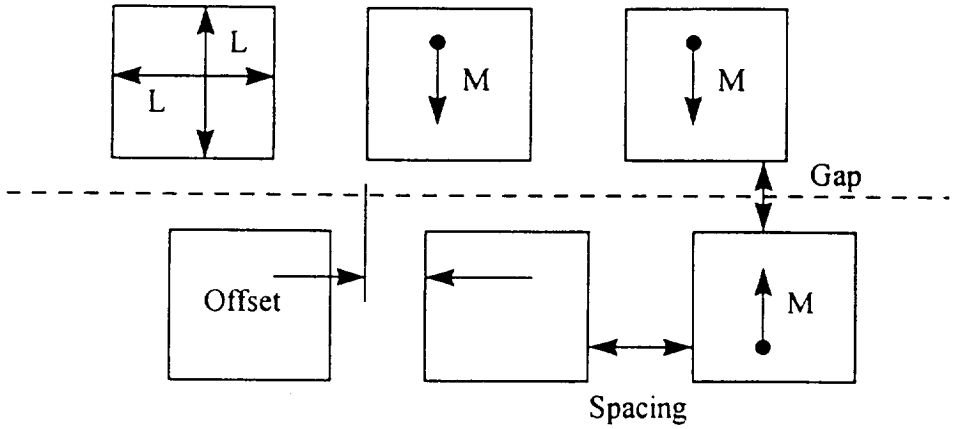


Figure 5 - Geometry of Computational Model

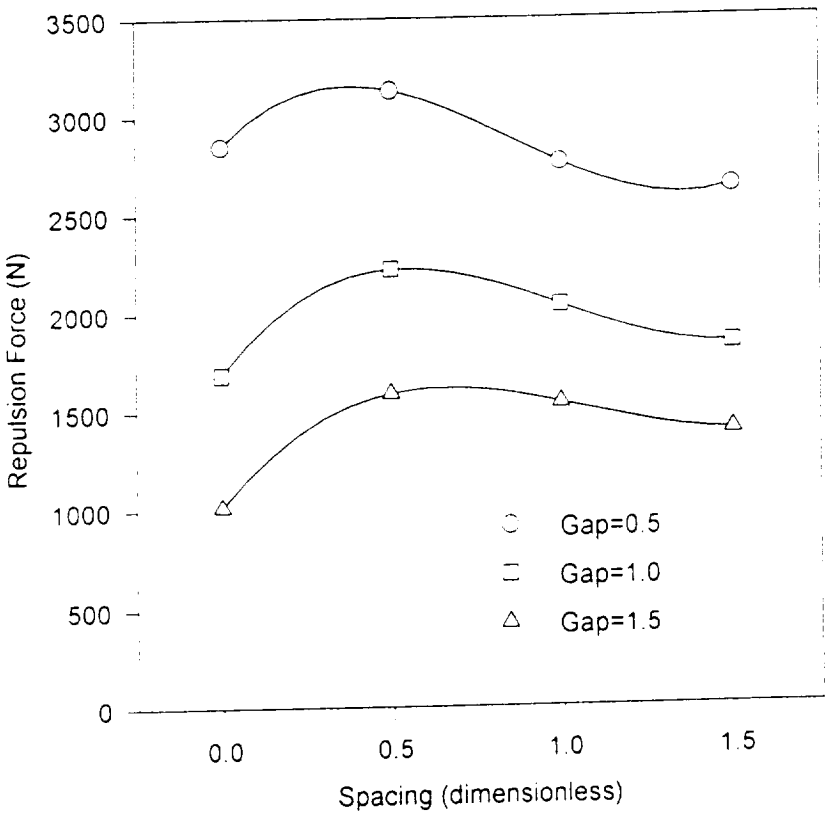


Figure 6 - Repulsion Force Versus Spacing Offset = 0

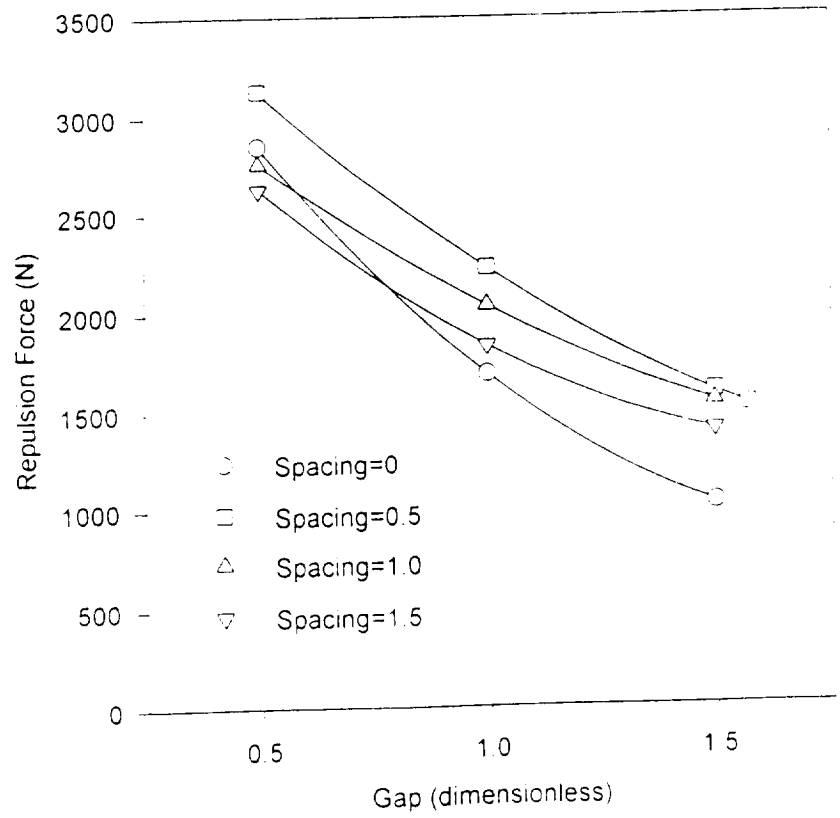


Figure 7 - Repulsion Force Versus Gap Offset = 0

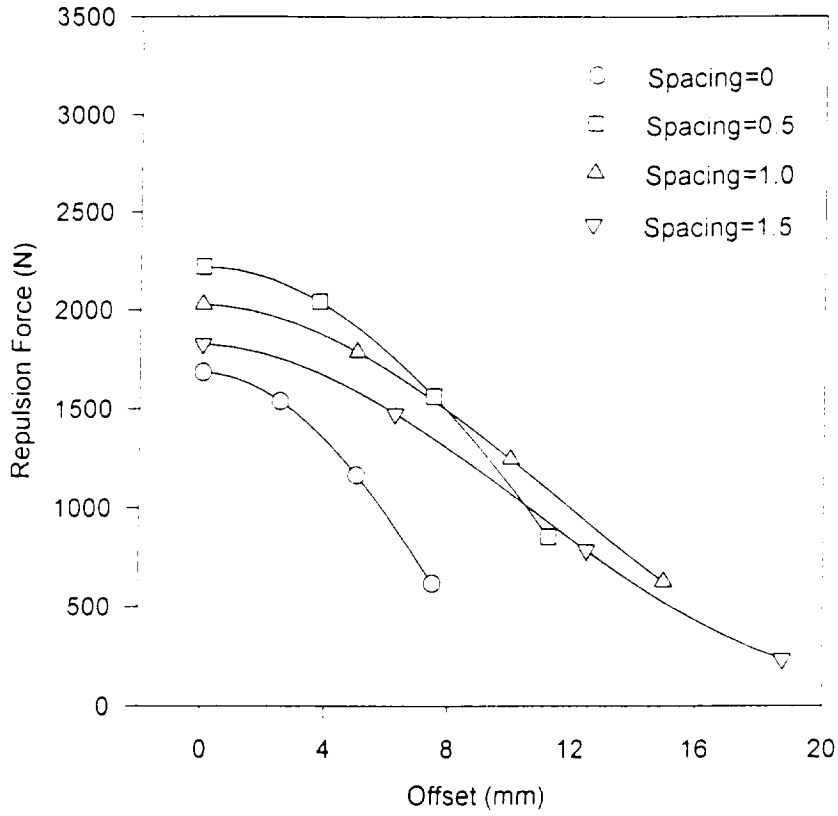


Figure 8 - Repulsion Force Versus Offset Gap = 1.0

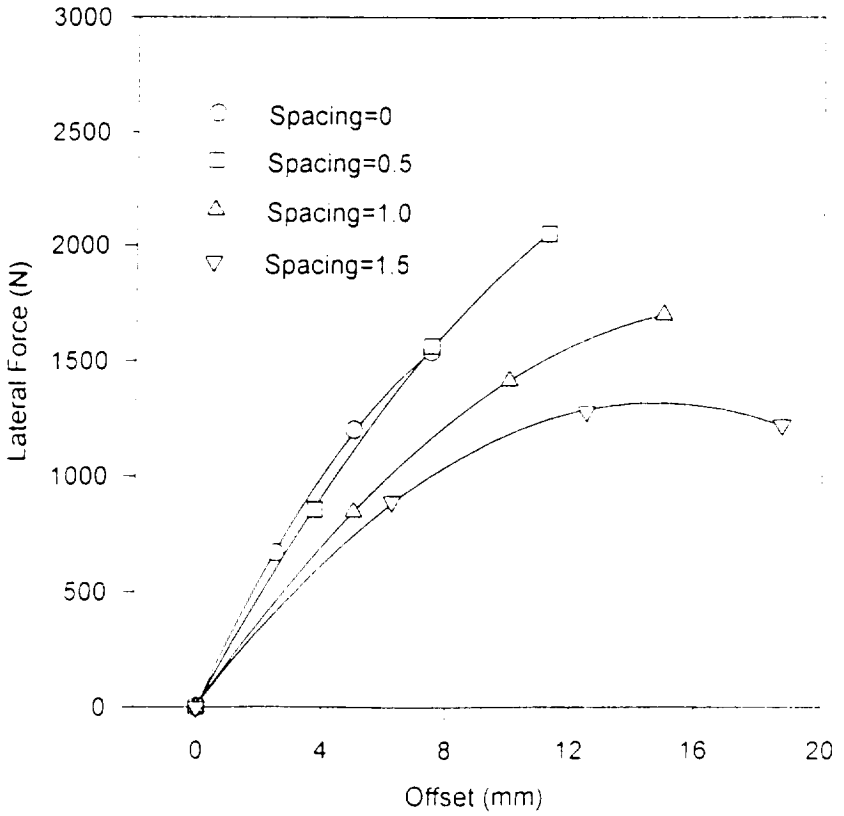


Figure 9 - Lateral Force Versus Offset Gap = 1.0